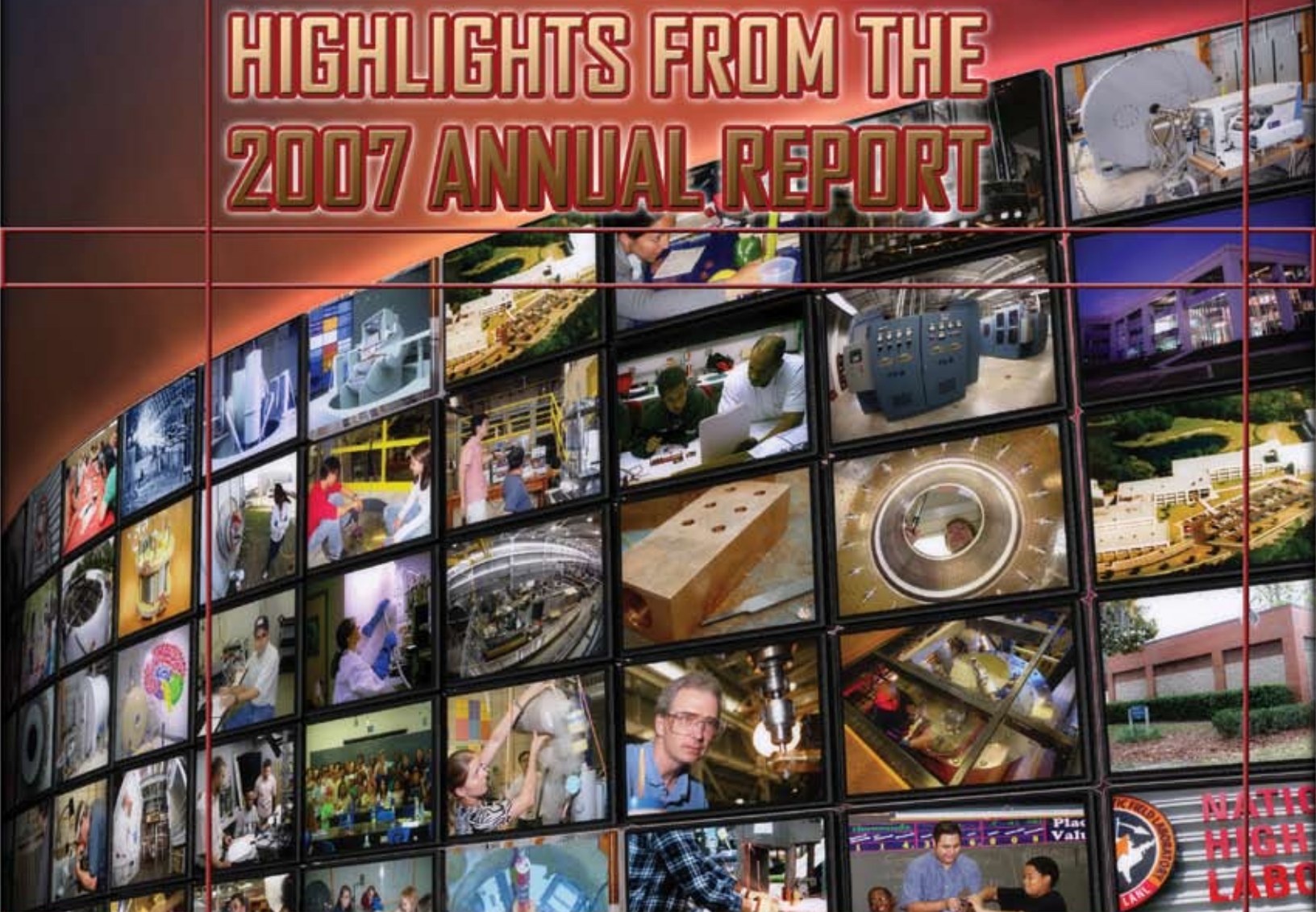


NATIONAL HIGH MAGNETIC FIELD LABORATORY

# MAG LAB REPORTS HIGHLIGHTS FROM THE 2007 ANNUAL REPORT



FLORIDA STATE UNIVERSITY    UNIVERSITY OF FLORIDA    LOS ALAMOS LAB  
SUPPORTED BY: THE NATIONAL SCIENCE FOUNDATION AND THE STATE OF FLORIDA






2	VOLUME 15 No.2	SPECIAL EDITION
3	<i>Introduction from the Director</i>	
5	LIFE SCIENCES	
11	CHEMISTRY	
19	MAGNET SCIENCE & TECHNOLOGY	
27	CONDENSED MATTER PHYSICS	

Published by:  
**National High Magnetic Field Laboratory**  
 1800 East Paul Dirac Drive  
 Tallahassee, Florida 32310-3706  
 Tel: 850 644-0311  
 Fax: 850 644-8350

**Mag Lab Director:** Greg Boebinger  
**Director of Public Affairs:** Susan Ray  
**Editing and Writing:** Amy Mast, Susan Ray  
**Graphic Design:** Savoy Brown

This document is available in alternate formats upon request. Contact Amy Mast for assistance. If you would like to be added to our mailing list, please write us at the address shown at left, call 850 644-1933, or email [winters@magnet.fsu.edu](mailto:winters@magnet.fsu.edu)

**Trying to reduce your carbon footprint?**



Sign up for an online subscription at <http://www.magnet.fsu.edu/mediacenter/publications/subscribe.aspx>

## 2007 Year in Review

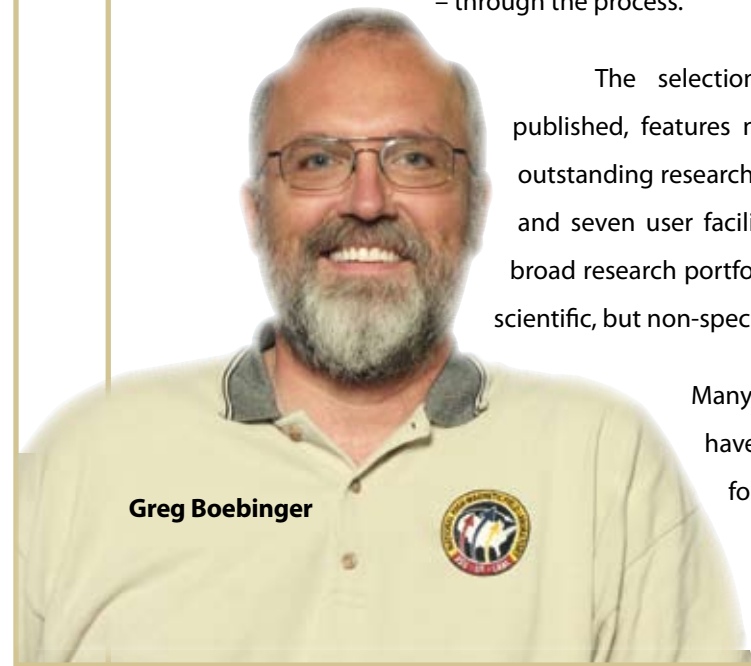
Welcome to our annual labor of love. At the end of each year, we ask Magnet Lab users and our research faculty at the Florida State University, University of Florida and Los Alamos National Lab to submit one-page abstracts of their MagLab research endeavors. And I'm sure that a spontaneous hue and cry arises from a thousand voices: "We love doing this again this year!" Surely, it's a fair exchange: Magnet time and expert on-site counsel, guidance and interpretation ... in exchange for a wee abstract.

Although your pure love of this annual chore would be reason enough, we also compile this information to get a snapshot summary of research experiments underway...a measure of activity that is different (and in many ways a leading indicator) of future publications in refereed journals.

We do in fact appreciate that a lot of work from our users and scientists goes into this issue. After we receive the reports they are reviewed by the MagLab Science Council, which has the difficult job of deciding which ones to forward to me for consideration as highlights. Of the 407 reports submitted, 43 were recommended by the council. Of that number, I picked 32: five in life sciences; seven in chemistry; seven in magnets and materials; and 13 in condensed matter science.

Sincere thanks goes to members of the Science Council for their thoughtful consideration. They are: Albert Migliori (chair), Rafael Bruschweiler, Mark Emmett, Lev Gor'kov, David Larbalestier, Denis Markiewicz, Dragana Popovic and Glenn Walter.

Thanks also go to Kathy Hedick for cat-herding all of the reports – and us – through the process.



**Greg Boebinger**

The selection criteria emphasizes research that is published, features new techniques for users, and showcases outstanding research that together spans all three MagLab sites and seven user facilities. As such, these reports represent the broad research portfolio of the MagLab in a concise format for a scientific, but non-specialist, audience.

Many reports containing preliminary results have been recognized as promising work to be followed closely in 2008.

Here are the vital statistics for the Research Reports:

- In 2007, 407 research reports were received in 17 categories, representing condensed matter physics, the life sciences, chemistry and magnet science and technology.
- 16% of the research activities in 2007 (64 reports) were already published in 2007, many in prominent journals.
- An additional 6% of the reports were accepted for publication; 11% were submitted for publication; and 40% have manuscripts in preparation.
- The majority of research projects were funded by the National Science Foundation, the Department of Energy, and the National Institutes of Health. Other funding organizations included: the American Chemical Society; American Heart Association, Engineering and Physical Sciences Research Council (UK), Human Frontiers Science Program, IBM, Japan Society for the Promotion of Science, Muscular Dystrophy Association, NASA, National Sciences and Engineering Research Council (Canada), Russian Academy of Science, U.S. Air Force Office of Scientific Research, U.S. Army, U.S. Geological Survey, U.S. Environmental Agency, and the U.S. Department of Veterans Affairs.
- The Magnet Lab's User Collaboration Grants Program (formerly and confusedly named the In-House Research Program) supported 48 of the 407 research activities and was the primary support for 24 projects. This grant program promotes collaborations between internal and external investigators, promotes bold but risky research efforts and provides initial seed money for new faculty, research staff and facility enhancements.

Finally, each of the 407 user reports and resulting publications is available on our Web site ([magnet.fsu.edu/usershub/publications](http://magnet.fsu.edu/usershub/publications)). You can search by user facility, journal, first author or principal investigator. In addition to the 2006 and 2007 user reports and publications, you can pull up all MagLab user reports since 2004 and all publications dating back to 2000.



ALBERT MIGLIORI



RAFAEL P. BRUSCHWEILER



MARK EMMETT



LEV GOR'KOV



DAVID LARBAESTIER



DENIS MARKIEWICZ



DRAGANA POPOVIC



GLENN WALTER

International researchers from such diverse fields as ecology to neuroscience are exploiting the extremely high mass specific sensitivity of the Magnet Lab's 1-mm HTS cryogenic probe to characterize rare samples found in ecosystems ranging from tropical rainforests to the Florida Keys. Often these active compounds can only be isolated in submilligram quantities hampering structure elucidation. In the report by Matthew *et al.*, the sensitivity of this probe was exploited to identify novel active chemotypes and pharmacophores produced by cyanobacteria. They found that extracts of *Lyngbya confervoides* collected from Ft. Lauderdale and the Florida Keys yielded novel protease inhibitors that are potent inhibitors of elastase. The use of this HTS 1-mm probe is expected to play an increasing role in drugs discovered from rare samples.

*This work was published in the Journal of Natural Products (2007).*

## EXPLOITING FLORIDIAN MARINE CYANOBACTERIA FOR DRUG DISCOVERY

S. Matthew (UF, Medicinal Chemistry); K. Taori (UF, Medicinal Chemistry); J.C. Kwan (UF, Medicinal Chemistry); V.J. Paul (Smithsonian Marine Station); H. Luesch (UF, Medicinal Chemistry)

### INTRODUCTION

There is an urgent need to identify novel active chemotypes and pharmacophores as leads for effective drug development in many therapeutic areas. Our research is based on the hypothesis that marine cyanobacteria are a potential source of novel bioactive compounds. There is substantial evidence for the large biosynthetic capacity of cyanobacteria to produce chemically diverse secondary metabolites of biomedical utility. Florida harbors possibly the most marine biodiversity in the continental United States, and therefore there is a high probability of discovering novel and intriguing structures. One major problem is that oftentimes only submilligram quantities of active components can be isolated, hampering structure elucidation.

### EXPERIMENTAL

<sup>1</sup>H, <sup>13</sup>C, and 2D NMR spectra for cyanobacterial metabolites were recorded on Bruker Avance NMR spectrometers (500 MHz, 2.5 mm probe; 600 MHz warm bore, 5 mm probe; 750 MHz, 2.5 mm probe) or Bruker Avance II 600 MHz spectrometer equipped with National High Magnetic Field Laboratory's 1 mm triple-resonance high-temperature superconducting (HTS) cryogenic probe.

### RESULTS AND DISCUSSION

Marine cyanobacteria of the genera *Symploca* and *Lyngbya* were collected off the coast of Florida, extracted and scrutinized for compounds with biomedical utility. Several extracts of *Lyngbya confervoides* collections from Ft. Lauderdale and the Florida Keys yielded novel protease inhibitors, lyngbyastatins 4–7 (Figure 1),<sup>1,2</sup> which displayed exceptional potency in inhibiting elastase. Active extract components were isolated by bioassay-guided fractionation and analyzed by NMR (Figure 1). Lyngbyastatins 5 and 6 were isolated in extremely low yield (0.47 and 0.17 mg, respectively), yet structure determination could be achieved thanks to the 1-mm HTS cryogenic probe.<sup>2</sup>

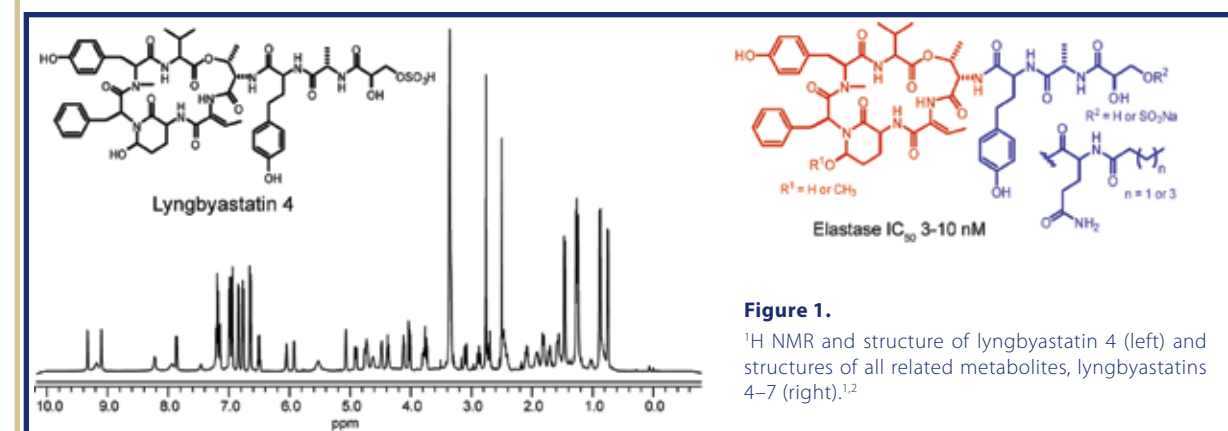


**Figure 1.**

<sup>1</sup>H NMR and structure of lyngbyastatin 4 (left) and structures of all related metabolites, lyngbyastatins 4–7 (right).<sup>1,2</sup>



**CONCLUSIONS**

Cyanobacteria continue to yield new bioactive metabolites. The 1-mm probe was essential for the successful NMR analysis.

**ACKNOWLEDGEMENTS**

Florida Sea Grant College Program NA06OAR4170014, External User Program of NHMFL at AMRIS (NSF), and J. Rocca.

**REFERENCES**

- [1] Matthew, S. *et al.*, *Journal of Natural Products*, **70**, 124-127 (2007).  
 [2] Taori, K. *et al.*, *Journal of Natural Products*, **70**, 1593-1600 (2007).

Multiply-labeled piscidin and HETCOR spectroscopy were successfully used to characterize the membrane-bound structure and tilt of piscidin 1 at high resolution. Access to high magnetic fields and low-E probes at the NHMFL enabled this work.

## HIGH-RESOLUTION NMR STRUCTURE AND TILT OF AMPHIPATHIC PISCIDIN AT THE WATER-BILAYER INTERFACE

Riqiang Fu (NHMFL), Eric Gordon (Pacific Lutheran University, Chemistry), Milton Truong (NHMFL), Mallorie Taylor (PLU), Jeff Ditto (PLU) and Myriam Cotten (PLU)

**INTRODUCTION**

This research combines several solid-state NMR techniques to obtain the high-resolution structure of membrane-bound piscidin 1 (p1)<sup>1</sup> and help establish relationships between its structural motif, interactions with biological membranes, potency, and mechanisms of action. Piscidin<sup>1</sup>, an amphipathic cationic antimicrobial peptide from fish, belongs to a large family of host-defense peptides that interact, at least initially, with cell membranes in order to perform their function. A bottleneck in this area of research is the lack of atomic level information on peptide-lipid interactions due to the challenges of performing traditional methods on physiologically relevant samples. Using solid-state NMR, we previously demonstrated that piscidin adopts an in-plane  $\alpha$ -helical conformation in the presence of hydrated phospholipid bilayers.<sup>2</sup>

Here, we used 2D HETCOR (*Heteronuclear correlation*) spectroscopy<sup>3</sup> to obtain the structure of membrane-bound piscidin. HETCOR correlates not only the orientation-dependent <sup>15</sup>N chemical shifts and <sup>1</sup>H-<sup>15</sup>N heteronuclear dipolar couplings as in PISEMA (*Polarization inversion spin exchange at the magic angle*)<sup>4</sup>, but also the <sup>1</sup>H chemical shift restraints from peptide planes. Similarly to PISEMA, HETCOR data can be directly analyzed to obtain tilt, polarity, and high-resolution structures of  $\alpha$ -helices.

**EXPERIMENTAL**

HETCOR experiments were carried out on the ultra-wide bore 900 MHz and Bruker Avance 600 MHz WB NMR spectrometers.

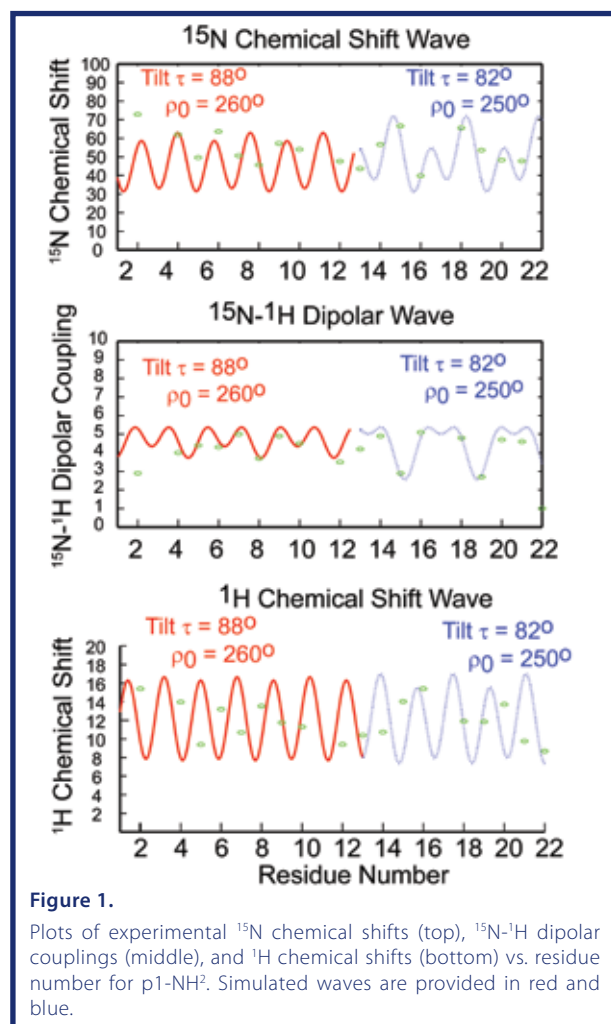


**Figure 1.**

Plots of experimental <sup>15</sup>N chemical shifts (top), <sup>15</sup>N-<sup>1</sup>H dipolar couplings (middle), and <sup>1</sup>H chemical shifts (bottom) vs. residue number for p1-NH<sup>2</sup>. Simulated waves are provided in red and blue.

**RESULTS AND DISCUSSION**

High-resolution HETCOR spectra were obtained from multiply <sup>15</sup>N-backbone labeled amidated p1 (p1-NH<sub>2</sub>) in the presence of aligned 3:1 phosphocholine/phosphoglycerate bilayers<sup>5</sup>. As shown in **Figure 1**, analysis of data from 18 sites of this 22-mer reveals the presence of two helical segments (tilts  $\tau = 88$  and  $82^\circ$ ) separated by a kink ( $\sim 6^\circ$ ) at Gly<sub>13</sub>. This kink may help one portion of the peptide insert more deeply in the hydrophobic lipid bilayer and this may be related to the mechanism of membrane disruption.

**CONCLUSIONS**

Multiply-labeled piscidin and HETCOR spectroscopy were successfully used to characterize the membrane-bound structure and tilt of piscidin 1 at high resolution. Access to high magnetic fields and low-E probes at the NHMFL facilitated this work.

**ACKNOWLEDGEMENTS**

We acknowledge support from the Dreyfus Foundation, Research Corporation, and Cambridge Isotope Laboratories.

**REFERENCES**

- [1] a) Silphaduang, U.; Noga, E.J. *Nature*. 2001, **414**, 268. b) Lauth, X *et al.* *J. Biol. Chem.* 2002, **277**, 5030.  
 [2] a) Chekmenev, E.Y., *et al.* *J. Am. Chem. Soc.* 2006, **128**, 5308. b) Chekmenev, E.Y., *et al.* *Biochim. Biophys. Acta.* 2006, **1758**, 1359.  
 [3] Fu, R.; Truong, M.; Saager, R. J.; Cotten, M.; Cross, T. A. *J. Magn. Reson.* 2007, **188**, 41.  
 [4] Wu, C.H.; Ramamoorthy, A.; Opella, S.J. *J. Magn. Reson. A.* 1994, **109**, 270.

2D HIMSELF spectra were recorded on bicelles containing uniformly <sup>15</sup>N-labeled cytochrome b<sub>5</sub> at 900 MHz with and without unlabeled cyt P450. Spectra are remarkably resolved and PISA wheels from the transmembrane region are well identifiable. Structural and dynamics changes in the rigid transmembrane region of cyt b<sub>5</sub> in the presence of cyt P450 are observed. These results will open new approaches to study the structure and dynamics of cyt b<sub>5</sub> as well as the cyt b<sub>5</sub>-cyt P450 complex.

## THE STRUCTURE AND DYNAMICS OF MEMBRANE-BOUND CYTOCHROME b<sub>5</sub> – CYTOCHROME P450 COMPLEX BY MEANS OF SOLID-STATE NMR SPECTROSCOPY

Kazutoshi Yamamoto, Jiadi Xu, Sang-Choul Im, Lucy Waskell, and Ayyalusamy Ramamoorthy (University of Michigan)

**INTRODUCTION**

Protein science in the post-genomic era is beginning to direct its course towards the elucidation of protein-protein interactions. Many biologically important protein-protein interactions, such as signal transduction, electron transport chain and photosynthesis, take place on the surface or across the lipid membrane of living cells. Despite their importance and ongoing investigative efforts, there have been very few reports on the protein structure determination of the complexes composed of protein-protein interactions and lipid bilayers. Practicable methods were deemed necessary to characterize the structure of complex protein systems due to the difficulties associated with membrane proteins in general and membrane protein-protein complexes in particular. We carried out the first studies

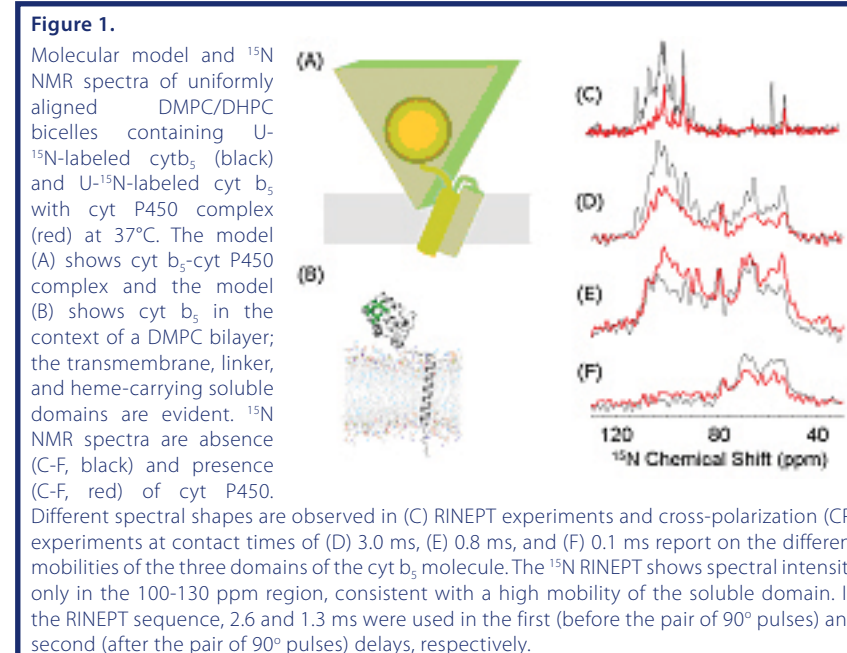
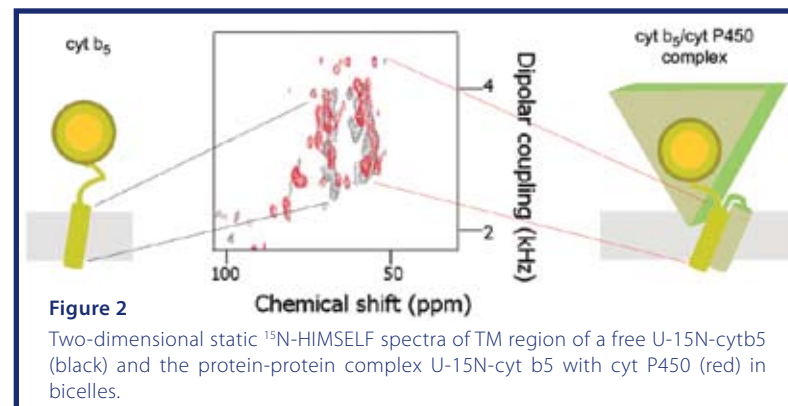


**Figure 1.**

Molecular model and <sup>15</sup>N NMR spectra of uniformly aligned DMPC/DHPC bicelles containing U-<sup>15</sup>N-labeled cytb<sub>5</sub> (black) and U-<sup>15</sup>N-labeled cyt b<sub>5</sub> with cyt P450 complex (red) at 37°C. The model (A) shows cytb<sub>5</sub>-cyt P450 complex and the model (B) shows cytb<sub>5</sub> in the context of a DMPC bilayer; the transmembrane, linker, and heme-carrying soluble domains are evident. <sup>15</sup>N NMR spectra are absence (C-F, black) and presence (C-F, red) of cyt P450. Different spectral shapes are observed in (C) RINEPT experiments and cross-polarization (CP) experiments at contact times of (D) 3.0 ms, (E) 0.8 ms, and (F) 0.1 ms report on the different mobilities of the three domains of the cytb<sub>5</sub> molecule. The <sup>15</sup>N RINEPT shows spectral intensity only in the 100-130 ppm region, consistent with a high mobility of the soluble domain. In the RINEPT sequence, 2.6 and 1.3 ms were used in the first (before the pair of 90° pulses) and second (after the pair of 90° pulses) delays, respectively.

on an intact mammalian membrane protein complex, rabbit cytochrome  $b_5$  (cyt  $b_5$ ) and cytochrome P450 2B4 (cyt P450), in a membrane bilayer environment by means of solid-state NMR at the atomic-level.<sup>1</sup> Cyt  $b_5$  activates the enzymatic function of cyt P450 to oxidize a wide variety of pharmaceutical compounds.<sup>2,2</sup> Since the oxidation of pharmaceutical compounds is of great importance to understanding their *in vivo* efficiency, there is considerable interest in understanding the interaction and function of the cyt  $b_5$ -cyt P450 complex. Cyt  $b_5$  is a 16.7 kDa protein consisting of three domains: a globular cytosolic domain consisting of a heme domain, a short linker region and a transmembrane domain. The transmembrane domain and linker region, which have been previously inaccessible to structural studies, are absolutely essential to activate cyt P450.



### EXPERIMENTAL

$^{15}\text{N}$  NMR was performed on a UWB 900MHz NMR spectrometer (at NHMFL) equipped with an NHMFL Low-E probe. The Low-E probe and higher magnetic field were useful for this study because the intact cyt P450 protein is heat sensitive. Spectral acquisition time was 18 hours for two-dimensional static  $^{15}\text{N}$ -HIMSELF<sup>3</sup> experiments at 30°C.

### RESULTS AND DISCUSSION:

2D HIMSELF spectra were recorded on bicelles containing uniformly  $^{15}\text{N}$ -labeled cyt  $b_5$  with and without unlabeled cyt P450 (Figure 2). Spectra are remarkably resolved and PISA wheels<sup>4</sup> from the TM region are clearly seen. Here, we found structural and dynamics changes in the rigid transmembrane region of cyt  $b_5$  in the presence of cyt P450. We expect these results will open new approaches to study the structure and dynamics of cyt  $b_5$  as well as the cyt  $b_5$ -cyt P450 complex.

### REFERENCES

- [1] U.H.N. Dürr, L. Waskell, A. Ramamoorthy, *Biochim. Biophys. Acta. Biomembranes*, doi:10.1016.
- [2] U.H.N. Dürr, K. Yamamoto, S.-C. Im, L. Waskell, A. Ramamoorthy, *J. Am. Chem.Soc.* 129(2007) 6670-6671.
- [3] K. Yamamoto, S.V. Dvinskikh, A. Ramamoorthy, *Chem. Phys. Lett.* 419(2006) 533-536. S.V. Dvinskikh, K. Yamamoto, A. Ramamoorthy, *J. Chem. Phys.* 125(2006) 034507.
- [4] J. Wang, J. Denny, C. Tian, S. Kim, Y. Mo, F. Kovacs, Z. Song, K. Nishimura, Z. Gan, R. Fu, J.R. Quine, T.A. Cross, *J. Magn. Reson.* 144(2000)162-167

It might come as a huge surprise that insect secretions could be the source of the next anti-cancer agent. In a report by the University of Florida Edison lab, that is exactly what they found. Using a highly sensitive HTS 1mm probe, they determined that the defensive secretion of *Parectatosoma mocquerysi*, a walkingstick insect from Madagascar, contains glucose, water, and a new monoterpene, parectadial, (4S)-(3-oxoprop-1-en-2-yl) cyclohex-1-enecarbaldehyde. Parectadial was also found to behave similarly to an anti-cancer agent, in that at a single concentration it inhibits the growth of several different established cancer cell lines. This study was made possible using the NHMFL's 1-mm HTS probe. This probe has proven to become an extremely efficient instrument for natural product discovery due to its high sensitivity when using extremely small amounts of material compared to conventional probes.

*This work was published in the Journal of Natural Products (2007).*

## PARECTADIAL: A NOVEL MONOTERPENE FROM PARECTATOSOMA MOCQUERYSI

A. T. Dossey (UF, Biochemistry); S. S. Walse (USDA Laboratory); O. Conle (Bolsterlang, Germany); A. S. Edison (UF, Biochemistry)

### INTRODUCTION

The NHMFL 1-mm HTS probe in AMRIS has been a great asset for natural product studies.<sup>1</sup> Using this probe,

the defensive secretion of *Parectatosoma mocquerysi* Finot 1897, a walkingstick insect from Madagascar, was determined to contain glucose, water, and a new monoterpene, parectadial, (4S)-(3-oxoprop-1-en-2-yl) cyclohex-1-enecarbaldehyde. This work demonstrates the utility of the 1-mm HTS probe and the value of walkingstick insects as sources of new bioactive compounds, and provides an analytical framework for identifying such substances.<sup>2</sup>

### EXPERIMENTAL, RESULTS AND DISCUSSION

*P. mocquerysi* was kept in culture by O. Conle (Figure 1), and the spray from 5 insects was collected and sent to the AMRIS facility for analysis. We used a variety of mass spectrometry, chromatography, and NMR techniques to show that the spray consists of glucose and a novel monoterpene that we named parectadial (Figure 2).

We showed by chemical synthesis and enantioselective gas chromatography and circular dichroism that insect produces only the "S" isomer that is shown in Figure 2. *Anisomorpha buprestoides*, a walkingstick found in Florida, produces a variable mixture of monoterpenes that have a 5 membered ring<sup>2,3</sup> rather than the 6 membered ring of parectadial.<sup>4</sup>

Based on similarities to other chemicals that have been shown to kill cancer cells, we have tested parectadial for anti-cancer activity. At a single concentration it inhibits the growth of several different cancer cell lines at the National Cancer Institute's 60 cell line screen and is currently in the second round of testing to evaluate a dose response.

### CONCLUSIONS

The NHMFL 1-mm HTS probe is an extremely efficient instrument for natural product discovery, because much less material is needed than for conventional probes.

### ACKNOWLEDGEMENTS

Bill Brey (NHMFL), Saikat Saha (NHMFL, now GE) Rich Withers (Bruker, now Varian), and Rob Nast (Bruker, now Varian) made the 1-mm HTS probe. Funding was from the HFSP, NIH, and NHMFL.

### REFERENCES

- [1] Brey, W. W., Edison, A. S., Nast, R. E., Rocca, J. R., Saha, S., and Withers, R. S. (2006) Design, construction, and validation of a 1-mm triple-resonance high-temperature-superconducting probe for NMR. *J Magn Reson* **179**, 290-3.
- [2] Dossey, A. T., Walse, S. S., Rocca, J. R., and Edison, A. S. (2006) Single Insect NMR: A New Tool to Probe Chemical Biodiversity. *ACS Chemical Biology* **1**, 511-514.
- [3] Zhang, F., Dossey, A. T., Zachariah, C., Edison, A. S., and Brusweiler, R. (2007) Strategy for automated analysis of dynamic metabolic mixtures by NMR. Application to an insect venom. *Analytical Chemistry* **79**, 7748-7752.
- [4] Dossey, A. T., Walse, S. S., Conle, O. V., and Edison, A. S. (2007) Parectadial, a Monoterpenoid from the Defensive Spray of *Parectatosoma mocquerysi*. *J Nat Prod* **70**, 1335-1338.

By utilizing two low energy fragmentation techniques on peptides, it is now possible to assign the peptide fragments as originating from either the N-terminus or C-terminus of the peptide parent, which will greatly facilitate the sequencing of peptides/proteins in the gas phase.

*This work was published in Analytical Chemistry (2007).*

## BURNING THE CANDLE AT BOTH ENDS: PROTEIN SEQUENCING FROM THE N- AND C-TERMINI

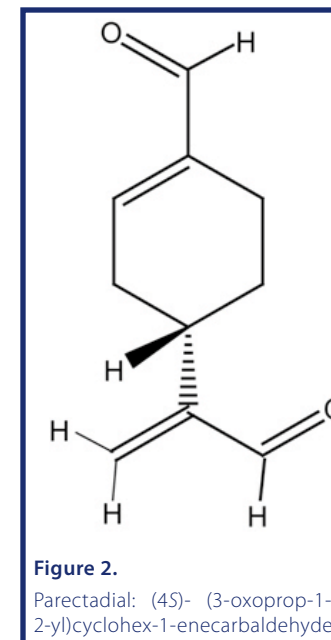
Yury O. Tsybin (NHMFL Tallahassee), Mark R. Emmett (NHMFL Tallahassee; FSU Chemistry & Biochemistry), Christopher L. Hendrickson (NHMFL Tallahassee; FSU Chemistry & Biochemistry), and Alan G. Marshall (NHMFL Tallahassee; FSU Chemistry & Biochemistry)

### INTRODUCTION

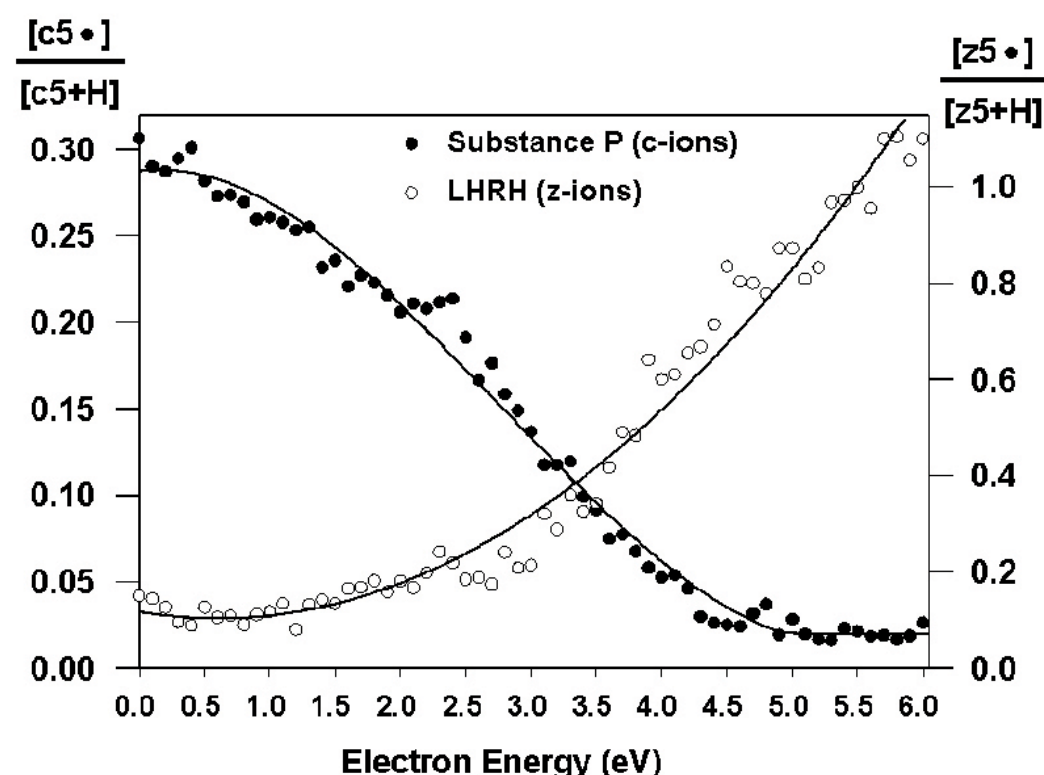
The most sensitive and informative way to determine the amino acid sequence of a protein is to slice it into segments with a suitable enzyme in solution, then "electrospray" it into the gas phase (i.e., remove all



**Figure 1.**  
Adult male *Parectatosoma mocquerysi*.







surrounding water molecules and add positive charges in the form of protons), and finally break it at various backbone positions and weigh the product peptides with a mass spectrometer. The mass difference between product peptides resulting from cleavage at consecutive linkages then identifies the amino acid by which they differ. Until now, it has not been possible to determine which end of the original peptide is contained in the charged fragment, leading to ambiguous identification.

### RESULTS AND DISCUSSION

NHMFL scientists have solved that problem by showing that a peptide breaks into two types of fragments, with relative abundances that depend on the energy of the electron "bullets" causing the fragmentation. Thus, by performing the fragmentation at each of two different electron energies, it is possible to determine whether the fragment ion is N- (amino-) terminal or C- (carboxyl-) terminal ("c" or "z" in the Figure). Protein identification is thus now twice as easy as before.

### ACKNOWLEDGEMENTS

This work was supported by the NSF National High-Field FT-ICR Mass Spectrometry Facility (DMR 00-84173), Florida State U., and NHMFL.

### REFERENCES

[1] Tsybin, Y. O.; *et al.*, *Anal. Chem.* **79**, 7596-7602 (2007).

Iron (Fe) is the most important transition metal in biology. Oxygen molecules ( $O_2$ ) bind to Fe in hemoglobin to be transported throughout the body via the bloodstream. Oxygen also is stored in muscle tissue by being bound to iron in myoglobin, another heme protein. In these cases, iron itself is not involved in chemical reactions. However, there also exist biomolecules, only recently discovered, known as non-heme iron enzymes. In these enzymes, oxygen molecules are activated by iron to create a highly reactive "ferryl" species,  $[FeO]^{2+}$ , which then reacts with various substrates to produce biologically important molecules. Very recently, stable small molecule analogs of this enzyme active species have been synthesized. We have now studied two of these molecules by high-frequency and high-field EPR (HFEP) at NHMFL. HFEP is uniquely suited for the study of these systems, due to their unusual electronic spin structure, and the best description to date of this aspect of the ferryl unit is now available. This information is of great importance to synthetic chemists in terms of helping them design better functional analogs to the enzymes. It is important also to biochemists in demonstrating the applicability of experimental methods present at NHMFL to the enzymes themselves. Lastly, the specific electronic structure information provided is important to computational chemists who are trying to understand the correlation between electronic structure and reactivity in both small molecules and in non-heme iron enzymes. Thus far, the enzymes are much more reactive than their synthetic analogs, but the basis for this is not well understood.

*The work was supported by the User Collaboration Grants Program and is currently in press in Inorganic Chemistry (2008).*

## HFEP STUDIES ON FERRYL COMPLEXES RELEVANT TO HEME AND NON-HEME IRON ENZYMES

K. Ray, J. England, L. Que, Jr. (U. of Minnesota, Chemistry); A. Ozarowski, D. Smirnov, J. Krzystek (NHMFL); J. Telsner (Roosevelt U., Chemistry)

### INTRODUCTION

Non-heme iron enzymes are widely found in biology and perform a broad range of functions, particularly activation of dioxygen and subsequent oxidative chemistry.<sup>1</sup> Considerable effort has been devoted to their spectroscopic characterization, by a variety of techniques including MCD and Mössbauer spectroscopies, as well as conventional EPR. In parallel, synthetic efforts have led to the isolation and characterization of model complexes for non-heme enzymes.<sup>2</sup>

The currently accepted model for the action of non-heme iron enzymes is via a ferryl ( $[Fe^{IV}O]^{2+}$ ) intermediate.<sup>1,2</sup> The electronic spin ground state of ferryl species can be either  $S = 2$ , or intermediate spin  $S = 1$ . Model complexes have thus far exhibited  $S = 1$  ground states;<sup>2</sup> however, surprisingly a  $S = 2$  ground state has been observed for the reactive ferryl intermediate in a non-heme iron enzyme.<sup>1</sup> The basis for this difference between enzyme and model compounds is of great interest. As a step toward understanding this difference, we have applied High Frequency EPR to study two stable ferryl complexes in the solid state:  $[FeO(tmc)(CH_3CN)](CF_3SO_3)_2$  (**1**) and  $[FeO(N4py)(CH_3CN)](CF_3SO_3)_2$  (**2**), where tmc is tetramethylcyclam (1,4,8,11-tetramethyl-1,4,8,11-tetraazacyclotetradecane) and N4py is bis(2-pyridylmethyl)bis(2-pyridyl)methylamine.<sup>2</sup>

### EXPERIMENTAL

The NHMFL Mm- and Sub-mm Wave Facility with the resistive ("Keck") 25-T magnet, and the EMR Facility with the superconducting 17-T magnet were used to study polycrystalline samples of **1** and **2**.

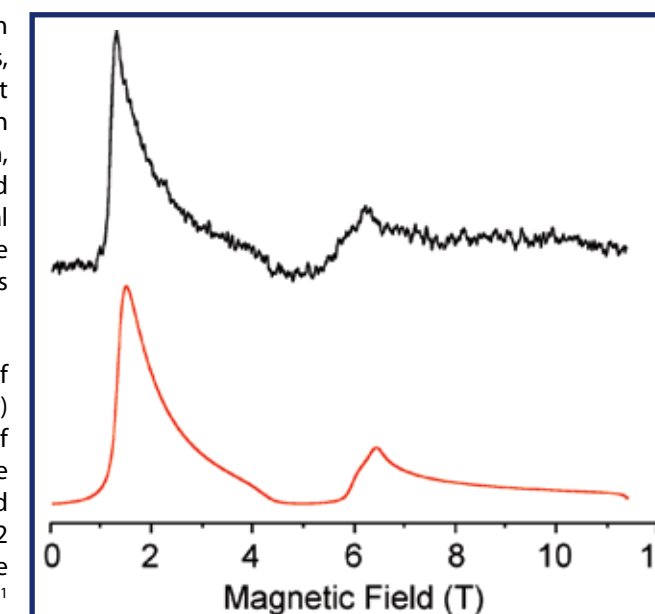


**Figure 1.** HFEP spectrum of **1** at 846 GHz and 5 K (black trace) with its powder-pattern simulation (red trace). Simulation parameters:  $S = 1$ ,  $D = +26.9 \text{ cm}^{-1}$ ,  $E = +0.095 \text{ cm}^{-1}$ ;  $g_{xy} = 2.1$ ;  $g_z = 2.04$ .

**RESULTS AND DISCUSSION**

An HFEPR spectrum of **1** is shown in Figure 1. The field vs. frequency dependence of the observed resonances confirm the triplet ( $S = 1$ ) ground spin state characterized by a zfs parameter  $|D|$  of  $\sim 27 \text{ cm}^{-1}$  and small rhombicity ( $E \sim 0$ ). A computer fit of this entire dataset provided complete spin Hamiltonian parameters as given in Fig. 1 caption. Similar results were obtained for **2**, although the zfs was significantly smaller ( $D = +22.0 \text{ cm}^{-1}$ ).

**CONCLUSIONS**

This study is the first application of HFEPR to the ferryl ( $[\text{Fe}^{\text{IV}}\text{O}]^{2+}$ ) ion, which is of great relevance to biological oxidation processes by iron-containing enzymes. From a technological and methodological point of view, the study is significant in that a new high value for zero-field splitting of the triplet spin state (nearly  $30 \text{ cm}^{-1}$ ) has been directly measured by HFEPR.

**ACKNOWLEDGEMENTS**

We thank the NHMFL-IHRP Program, Roosevelt University, and NIH (GM-33162 to LQ) for support.

**REFERENCES**

- [1] Krebs, C., *et al.*, *Acc. Chem. Res.* **40**, 484-492 (2007).  
 [2] Costas, M., *et al.*, *Chem. Rev.* **104**, 939-986 (2004).

Polymeric heterometallic compounds with properties potentially useful in the areas of magnetism, catalysis and electrical conductivity have been extensively studied in recent years. While important from a theoretical viewpoint, they may also give insight into the metal-metal interactions in biological systems like metalloenzymes that contain exchange-coupled paramagnetic metal ions. In this work, a supramolecular system containing infinite chains of binuclear anions  $[\text{Mn}_2(\text{succ})_2\text{Cl}_2]^{2-}$  (succ is the dianion of succinic acid) was synthesized. These chains are linked together by  $[\text{Cu}(\text{en})_2]^{2+}$  cations (en=ethylenediamine) to form an extended two-dimensional network.

Spectra expected for the anions and cations above were observed in high-field and -frequency EPR. However, additional weak signals were also seen that allowed to prove the presence of 8% of a 'swapped' system containing  $[\text{MnCu}(\text{succ})_2\text{Cl}_2]^{2-}$  anions and  $[\text{Mn}(\text{en})_2]^{2+}$  cations. These species eluded detection by x-ray crystallography. On the other hand, large zero-field splitting in binuclear Mn-Cu and Mn-Mn fragments rendered classical EPR useless. High-field and -frequency EPR is thus the only method indicating this interesting imperfectness of the synthetic method applied.

*This work is currently in press in Inorganic Chemistry (2008).*

## DIRECT SYNTHESIS, CRYSTAL STRUCTURES, HIGH-FIELD EPR AND MAGNETIC STUDIES OF HETEROMETALLIC POLYMERS CONTAINING MN(II) CARBOXYLATES INTERCONNECTED BY $[\text{Cu}(\text{en})_2]^{2+}$

V. G. Makhankova, A. O. Beznischenko, V. N. Kokozay (Kiev U., Chemistry); R. I. Zubatyuk, O. V. Shishkin (National Academy of Sciences, Kharkiv, Ukraine); J. Jezierska (Wroclaw U., Poland, Chemistry); A. Ozarowski (NHMFL)

**INTRODUCTION**

A novel synthetic strategy has been developed to directly obtain heterometallic polymeric coordination complexes in a 'one-pot' reaction. In this work the magnetic properties and High-Field EPR spectra of the compound  $[\text{Cu}(\text{en})_2][\text{Mn}_2(\text{succ})_2\text{Cl}_2]$  containing chains of dimeric  $[\text{Mn}_2(\text{succ})_2\text{Cl}_2]^{2-}$  anions linked by  $[\text{Cu}(\text{en})_2]^{2+}$  cations, (en = ethylene diamine), were studied.

**EXPERIMENTAL**

High-frequency EPR spectra up to 413 GHz were recorded on the transmission spectrometer at the EMR facility of the NHMFL. Magnetic susceptibility data of a powdered sample were measured with a SQUID magnetometer (Quantum Design MPMSXL-5) over the temperature range 1.8–300 K at the magnetic induction of 0.5 T.

**RESULTS AND DISCUSSION**

The dominant feature of the low-temperature high-field EPR spectra was an axially-symmetric spin-triplet ( $S=1$ ) signal characterized by isotropic g factor equal to 2 and the zero-field splitting parameter D of  $-3.046 \text{ cm}^{-1}$ . A  $D_{\text{Mn}}$  value for separate Mn(II) ions ( $S=5/2$ ) of  $+0.38 \text{ cm}^{-1}$  was deduced from these data and satisfactorily reproduced

by using a Density Functional Theory calculation<sup>1</sup> that resulted in  $D_{\text{Mn}} = +0.32 \text{ cm}^{-1}$ . Additional signals seen in EPR spectra as well as magnetic susceptibility data allowed to conclude that the 'one-pot' synthetic method produced 92% of the intended complex  $[\text{Cu}(\text{en})_2][\text{Mn}_2(\text{succ})_2\text{Cl}_2]$ , while in the remaining 8% the Mn(II) and Cu(II) ions were 'swapped' to form a  $[\text{Mn}(\text{en})_2][\text{MnCu}(\text{succ})_2\text{Cl}_2]$  system. The magnetic susceptibilities of the main complex ( $\chi$ ) and that of the 'swapped' system ( $\chi^{\text{sw}}$ ) were expressed as

$$\chi = \frac{Ng_{\text{Cu}}^2\beta^2}{3kT} \frac{\sum_{S=0}^5 (2S+1)(S+1)S \exp(-J_{\text{Mn-Mn}}S(S+1)/2kT)}{\sum_{S=0}^5 (2S+1) \exp(-J_{\text{Mn-Mn}}S(S+1)/2kT)} + \frac{Ng_{\text{Cu}}^2\beta^2}{3kT} \frac{3}{4} \quad \chi^{\text{sw}} = \frac{N\beta^2}{3kT} \frac{30g_{\text{Mn}}^2 + 84g_{\text{Cu}}^2 \exp(-3J_{\text{Cu-Mn}}/kT)}{5+7 \exp(-3J_{\text{Cu-Mn}}/kT)} + \frac{N\beta^2 g_{\text{Mn}}^2}{3kT} \frac{35}{4}$$

and the exchange integral  $J_{\text{Mn-Mn}}$  magnitude of  $32 \text{ cm}^{-1}$  was found from fitting procedures. The DFT calculation ('broken-symmetry' approach) resulted in  $J_{\text{Mn-Mn}} = 44 \text{ cm}^{-1}$ , in a reasonable agreement with experiment.

**CONCLUSIONS**

Magnetic susceptibility measurements and high-frequency EPR studies proved the absence of exchange interactions between  $[\text{Cu}(\text{en})_2]^{2+}$  units and Mn<sup>II</sup>-carboxylate anions, while the manganese ions in the dimeric anion were found to be exchange-coupled. The single-ion  $D_{\text{Mn}}$  was satisfactorily reproduced by a DFT calculation using the ORCA software package,<sup>1</sup> as was the exchange integral magnitude  $J_{\text{Mn-Mn}}$ . The magnetic and EPR results indicate that the 'one-pot' synthesis was highly, but not perfectly efficient in putting manganese and copper ions in desired locations.

**ACKNOWLEDGEMENTS**

This work was supported in part by INTAS (project YS 05-109-4488) and by the NHMFL. The NHMFL is funded by the NSF through the Cooperative Agreement No. DMR-0084173 and the State of Florida.

**REFERENCES**

- [1] Neese, F. ORCA – an ab initio, DFT and Semiempirical Program Package, Version 2.6-04, 2007; Universität Bonn: Bonn, Germany

Instrumentation at the Magnet Lab is allowing for the study of diffusion on the nanoscale in model systems. Sanders and Vasenkov have performed non-invasive studies of lipid self-diffusion in membranes on the nanoscale using NMR spectroscopy combined with pulsed field gradients up to 35 T/m gradient amplitudes (see Report #123, <http://www.magnet.fsu.edu/usershub/publications/researchreportonline.aspx>). Their studies demonstrate that it is possible to monitor anomalous diffusion in lipid bilayers deposited on oriented glass stacks at 750 MHz and over length scales as small as 100 nm. Using another approach, the Bowers lab has developed novel approaches to follow diffusion of hyperpolarized Xe atoms as they near the openings of self-assembled L-Alanyl-L-Valine dipeptide nanotubes. In the current report, Cheng and Bower report a new method to provide greater accuracy in rate constant determination, and facilitate measurement of smaller exchange rate constants. This allows for the determination of slower exchange processes or longer diffusion time/length scales for in the depth characterization of nanotubes or nanoporous materials in general.

*This work was supported by the Magnet Lab's User Collaboration Grants Program and published in the Journal of the American Chemical Society (2007).*

## INTERRUPTED GAS FLOW TO ENHANCE CROSS-PEAK NMR SIGNALS IN HYPERPOLARIZED XENON GAS: A NEW TECHNIQUE FOR STUDYING NANOSCALE DIFFUSION

C.-Y. Cheng, J.P. Pfeilsticker and C.R. Bowers, Department of Chemistry, University of Florida

**INTRODUCTION**

In our recent JACS article<sup>1</sup> we presented a study of the exchange kinetics of Xe atoms localized near the openings of self-assembled L-Alanyl-L-Valine (AV) dipeptide nanotubes<sup>2,3</sup> utilizing continuous-flow hyperpolarized 2D-EXSY NMR. In CFHP 2D-EXSY, hyperpolarized gas is transported from the optical pumping cell to the sample space at a constant flow rate, enabling the rapid acquisition of 2D spectra with enhanced sensitivity. In deriving the expressions for the cross-peak signals under flow conditions, we noted that the finite residence time of the hyperpolarized gas inside the sample space may suppress diagonal- and cross-peak signals, and we suggested that the undesired signal suppression could be mitigated simply by interrupting the gas flow during the mixing time of the 2D-EXSY pulse sequence.<sup>1</sup> Here we present the dramatic experimental confirmation of this effect in AV.



**EXPERIMENTAL**

A 15mg AV sample was evacuated in-situ to  $\sim 10^{-5}$  torr at 100°C for 2-3 hours prior to experiments. The gas mixture consisted of 2%  $^{129}\text{Xe}$ , 2%  $\text{N}_2$  and 96%  $^4\text{He}$  at a total pressure of 4600mbar. A fractional nanotube occupancy of  $\theta = 0.047$  was inferred from the Xe shift tensor. The continuous-flow hyperpolarized  $^{129}\text{Xe}$  NMR setup is the same as that described in Ref. 1, except for one modification: the outlet of the sample space was connected to a two-way solenoid valve. An auxiliary TTL gate on the Bruker spectrometer was used to switch the solenoid valve from the pulse program to stop the flow of gas.

**RESULTS AND DISCUSSION**

The CF and IF mode hyperpolarized  $^{129}\text{Xe}$  2D-EXSY spectra acquired in AV nanotubes at  $\tau_m = 1\text{s}$  are presented below. The continuous-flow sequence barely yielded any cross-peaks. In contrast, the IF mode spectrum exhibits intense gas phase diagonal and exchange cross-peak signals. Thus, by interrupting the gas flow during the EXSY pulse sequence, the cross-peak signals were enhanced by a factor of  $\sim 60$ .<sup>4</sup>

**CONCLUSIONS**

Our new method will provide greater accuracy in rate constant determination, and facilitate measurement of smaller exchange rate constants. It may also be applicable to other hyperpolarized species such as  $^1\text{H}$  or  $^{13}\text{C}$  generated from parahydrogen or DNP. The ability to probe longer mixing times will facilitate extension of hyperpolarized 2D-EXSY to slower exchange processes or longer diffusion time/length scales for characterization of nanotubes or nanoporous materials in general.

**ACKNOWLEDGEMENTS**

Construction of the Xenon-129 polarizer was supported by the NHMFL In-House Research Program and UF.

**REFERENCES**

- [1] C.-Y. Cheng and C.R. Bowers, *J. Am. Chem. Soc.* **129**, 13997-14002 (2007).
- [2] I. Moudrakovski *et al.* *Proc. Natl. Acad. Sci. U.S.A.* **101**, 17924-17929 (2004).
- [3] C.-Y. Cheng and C.R. Bowers, *ChemphysChem*, **8** 2077 – 2081 (2007).
- [4] C.-Y. Cheng, J.P. Pfeilsticker and C.R. Bowers, *J. Am. Chem. Soc.* **130**, 2390-2391 (2008)

A significant and clever advance in MAS NMR, "The probe currently outperforms commercial probes we have tested as well as results published for other designs." Adds capability to the user program and the field as well. It has already been used for new measurements described by the authors in another report.

• This work was supported by the User Collaboration Grants Program and was published in *Magnetic Resonance in Chemistry* (2007).

## LOW-E MAGIC ANGLE SPINNING PROBE FOR BIOLOGICAL SOLID STATE NMR AT 750 MHZ

**P.L. Gor'kov, W.W. Brey (NHMFL/FSU); S. McNeill (UF Electrical and Computer Engineering); J.R. Long (UF Biochemistry and Molecular Biology)**

**INTRODUCTION**

Crossed-coil NMR probes are a useful tool for reducing sample heating for biological magic angle spinning (MAS) NMR. In a crossed-coil probe, the higher frequency  $^1\text{H}$  field, which is the primary source of sample heating in conventional probes, is produced by a separate low-inductance resonator. Because a smaller driving voltage is required, the electric field across the sample and the resultant heating is reduced. In a commercial

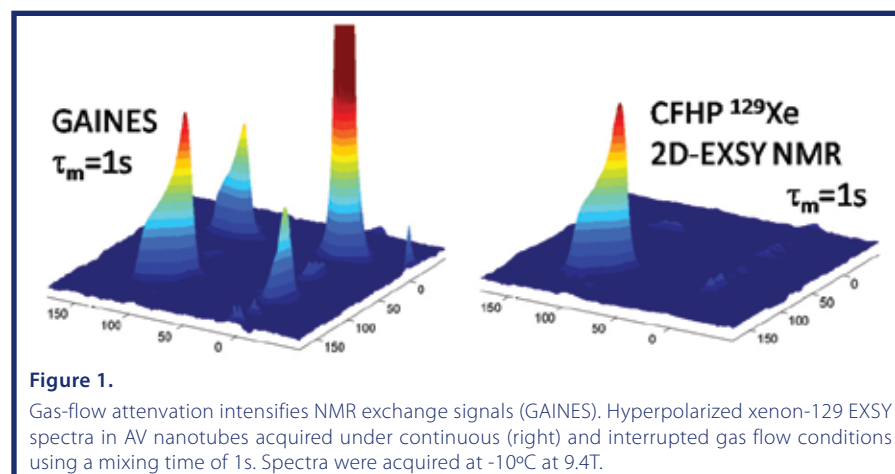


Figure 1.

Gas-flow attenuation intensifies NMR exchange signals (GAINES). Hyperpolarized xenon-129 EXSY spectra in AV nanotubes acquired under continuous (right) and interrupted gas flow conditions using a mixing time of 1s. Spectra were acquired at  $-10^\circ\text{C}$  at 9.4T.

implementation, the  $^1\text{H}$  coil is placed inside the low-frequency solenoid<sup>1</sup>. Last year we successfully developed a MAS probe based on the alternative approach of placing the  $^1\text{H}$  resonator outside the solenoid (Figure 1). Because the solenoid can then be smaller and better separated from the  $^1\text{H}$  resonator, we expect that this approach will give improved sensitivity and allow higher  $B_1$  fields without arcing between the two coils. This dual resonator approach, named "Low-E," was originally developed to reduce heating in samples of mechanically aligned membranes<sup>2</sup>, where it allowed the use of larger samples that were required to obtain sufficient NMR signal. The study of inherently dilute systems, such as proteins in lipid bilayers, via MAS techniques also requires large sample volumes at high field to obtain spectra with a sufficient signal to noise ratio under physiologically relevant conditions. This year we tested the probe under a variety of conditions, fine tuning design elements to improve proton decoupling fields. The probe currently outperforms commercial probes we have tested as well as results published for other designs. In particular, due to the larger volume of the rotor, we are able to examine structures in membrane associated peptides at physiologically relevant concentrations.

**METHODS**

The probe was thoroughly characterized in order to determine maximum achievable  $B_1$  fields, homogeneity of the  $B_1$  fields, RF efficiencies, RF heating, frictional heating under MAS, spectral linewidths, and signal/noise on standard compounds. Working with Revolution NMR (Ft. Collins, CO), we were able to obtain rotors which have thinner walls and spin stably at 12 kHz, allowing us to pack more sample into the rotors. To increase robustness on the proton channel, capacitors were added in parallel to reduce voltages at individual points. This caused a small decrease in RF efficiency but allows us to operate for long periods of time with high proton decoupling.

**RESULTS AND DISCUSSION**

Under normal operating conditions, a  $^1\text{H}$   $B_1$  field of 93 kHz and homogeneity ( $810^\circ/90^\circ$ ) of 93% can be obtained with a sample length of 8.4mm corresponding to a volume of 80 $\mu\text{l}$ . With a higher power amplifier, we should be able to reach 110 kHz based on bench measurements.  $^{13}\text{C}$   $B_1$  fields of  $> 71$  kHz homogeneity ( $810^\circ/90^\circ$ ) of 89% are routinely observed. Under full  $^1\text{H}$  decoupling for long periods of time, sample heating due to the high RF field is minimal even for sample containing physiological levels of salt. The power handling characteristics,  $B_1$  fields, and homogeneities make this an ideal probe for the full range of solid state NMR experiments, including sequences which use extended periods of continuous RF pulsing on both channels. We recently published a paper describing design considerations as well as some initial results<sup>3</sup>. A more detailed manuscript demonstrating the probe's capabilities with a variety of samples and pulse sequences is nearing completion.

**REFERENCES**

- [1] Doty, F.D., *et al.*, *J. Magn. Reson.* **182** (2006) 239-253.
- [2] Gor'kov, P.L., *et al.*, *J. Magn. Reson.* **185** (2007) 77-93.
- [3] McNeill, S.A., Gor'kov, P.L., Struppe, J., Brey, W.W., and Long, J.R., *Magn. Reson. Chem.* **45**(2007) S209-S220.

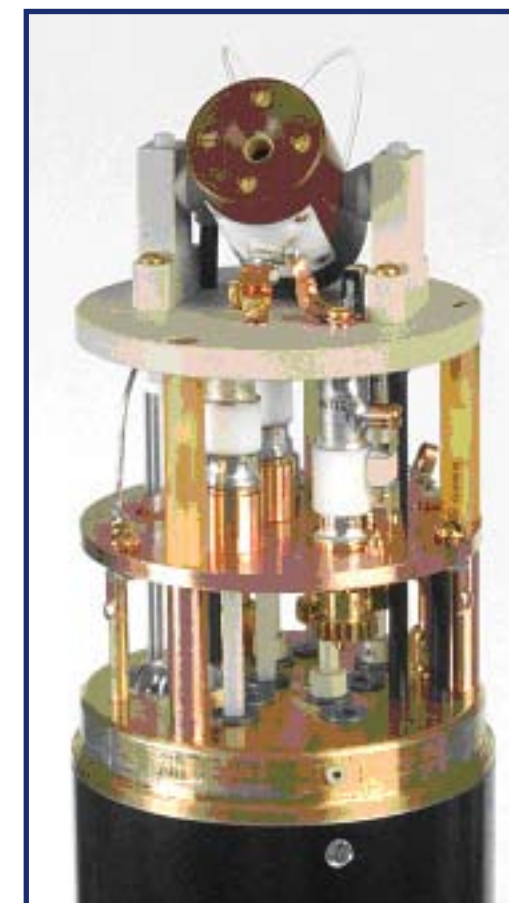


Figure 1.

Low E probe showing stator and tuning network.



This report identifies the components of crude oil that readily dissolve in water (both fresh and salt water). This information is important in tracing the source and remediation of oil spills in the environment. This could be of great importance in spills that occur in the water table.

• This work was published in *Environmental Science & Technology* (2007).

## WHICH COMPONENTS OF CRUDE OIL DISSOLVE IN WATER?

Lateefah Stanford (FSU Chemistry & Biochemistry), Sunghwan Kim (Korean Basic Science Institute, Korea), Geoffrey C. Klein (FSU Chemistry & Biochemistry), Donald F. Smith (FSU Chemistry & Biochemistry), Ryan P. Rodgers (NHMFL Tallahassee; FSU Chemistry & Biochemistry), and Alan G. Marshall (NHMFL Tallahassee; FSU Chemistry & Biochemistry)

### RESULTS AND DISCUSSION

The first step in understanding petroleum crude oil spills is to identify which chemical components dissolve in water. Here, we use ultrahigh-resolution magnet-based mass spectrometry to resolve and identify, for the first time, thousands of different chemical components of crude oil and water exposed to that oil.<sup>1</sup> Of the 7,000+ acidic species identified in South American crude oil, surprisingly many are water-soluble, and many more in pure water than in seawater (see Figure, Top: crude oil. Bottom: water-soluble components). Water solubility depends on molecular weight, size, and heteroatom

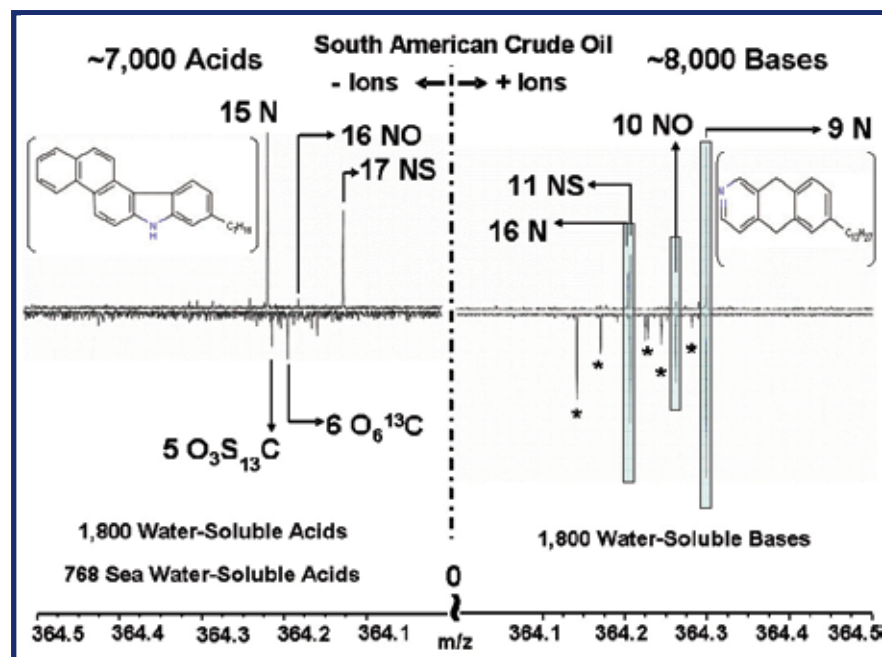
(nitrogen, oxygen, sulfur) content. Acidic oxygen-containing chemicals are most prevalent in the water-solubles, whereas acidic nitrogen-containing chemicals are least soluble. In contrast, basic nitrogen-containing chemicals are water-soluble. (Peaks noted with an asterisk in the distilled water-soluble bases portion of the Figure are nitrogen/oxygen/sulfur-containing compounds too dilute to be detected in the parent oil.) Possible structures are shown for two of the chemical components.

### ACKNOWLEDGEMENTS

This work was supported by the NSF National High-Field FT-ICR Mass Spectrometry Facility (DMR 06-54118), Florida State U., and NHMFL.

### REFERENCES

[1] Stanford, L.A. *et al.*, *Environ. Sci. Technol.* **41**, 2696-2702 (2007).



Technique development to improve both FT-ICR mass spectral signal-to-noise ratio (at fixed resolving power) and resolving power (at fixed signal-to-noise ratio). The time-domain signal duration increases by up to a factor of 2 or more. Mechanism is under investigation.

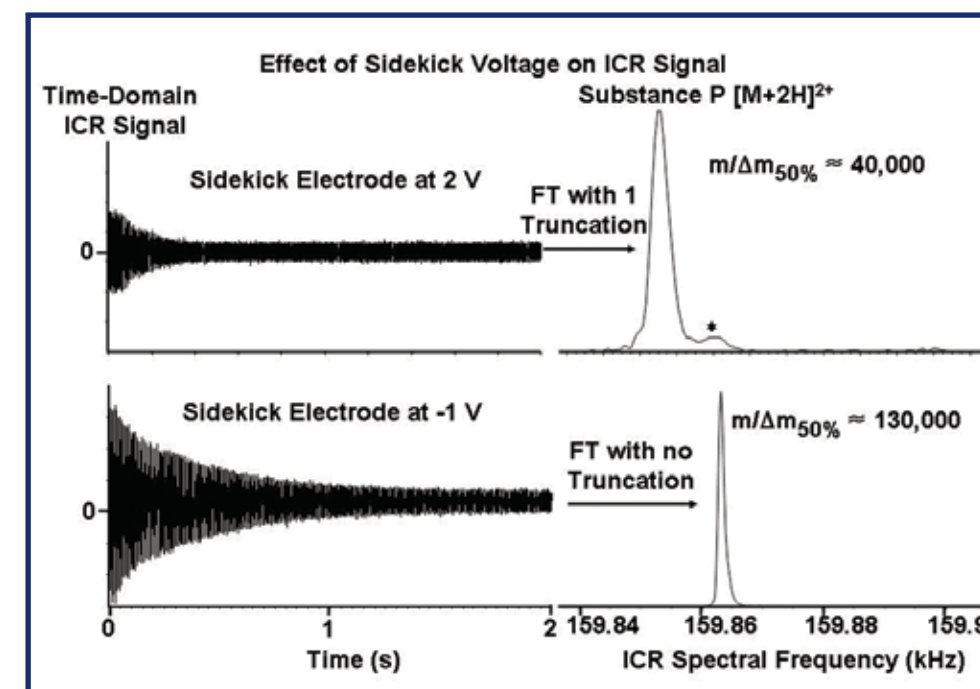
• This work was published in *Analytical Chemistry* (2007).

## MODIFICATION OF TRAPPING POTENTIAL BY INVERTED SIDEKICK ELECTRODE VOLTAGE DURING DETECTION EXTENDS TIME-DOMAIN SIGNAL DURATION FOR SIGNIFICANTLY ENHANCED FOURIER TRANSFORM ION CYCLOTRON RESONANCE MASS RESOLUTION

Sunghwan Kim (Korean Basic Science Institute, Korea), Myoung Choul Choi (Korean Basic Science Institute, Korea), Seungyoung Kim (Korean Basic Science Institute, Korea), Manhoi Hu (Korean Basic Science Institute, Korea), Jong Shin Yoo (Korean Basic Science Institute, Korea), Hyun Sik Kim (Korean Basic Science Institute, Korea), Greg T. Blakney (NHMFL Tallahassee), Christopher L. Hendrickson (NHMFL Tallahassee; FSU Chemistry & Biochemistry), and Alan G. Marshall (NHMFL Tallahassee; FSU Chemistry & Biochemistry)

### RESULTS AND DISCUSSION

Applying an inverted voltage to the "sidekick" electrodes during ion cyclotron resonance detection improves both Fourier transform ion cyclotron resonance (FT-ICR) mass spectral signal-to-noise ratio (at fixed resolving power) and resolving power (at fixed signal-to-noise ratio)<sup>1</sup>. The time-domain signal duration increases by up to a factor of 2 or more. The method has been applied to 7 T FT-ICR MS of electrosprayed positive ions from



substance P (see Figure) and human growth hormone protein (~22,000Da,  $m/\Delta m_{50\%} \approx 200,000$ ), without the need for pulsed cooling gas inside the ICR trap. The modification can be easily adapted to any FT-ICR instrument equipped with sidekick electrodes. The present effects are shown to be comparable to electron field modification by injection of an electron beam during ICR detection, reported by Kaiser and Bruce<sup>2</sup>. Although the exact mechanism is not fully understood, computer simulations show that a flattening of the radial potential gradient along the magnetic field direction and formation of an inverted local potential gradient well in the ICR trap may contribute to the effects. This study provides not only a way to enhance the quality of FT-ICR mass spectra but also offers insight into understanding of ion motions inside an ICR ion trap.

**ACKNOWLEDGEMENTS**

We thank John P. Quinn for help in interfacing the Predator data station to the Bruker FT-ICR mass spectrometer. We also thank Drs. Jung-Keun Suh and Young-Lan Jung for providing protein standard samples. This work was supported by the NSF National High-Field FT-ICR Mass Spectrometry Facility (DMR 06-54118), Florida State U., NHMFL, and the Korean Basic Science Institute.

**REFERENCES**

- [1] Kim, S. *et al.*, *Anal. Chem.* **79**, 3757-3580 (2007).  
 [2] Kaiser, N. K. *et al.*, *Anal. Chem.* **77**, 5973-5981 (2005).

The combination of specific ionization techniques and accurate mass, high resolution Fourier transform ion cyclotron mass spectrometry permit the assignment of chemical composition and structure prediction based solely upon mass.

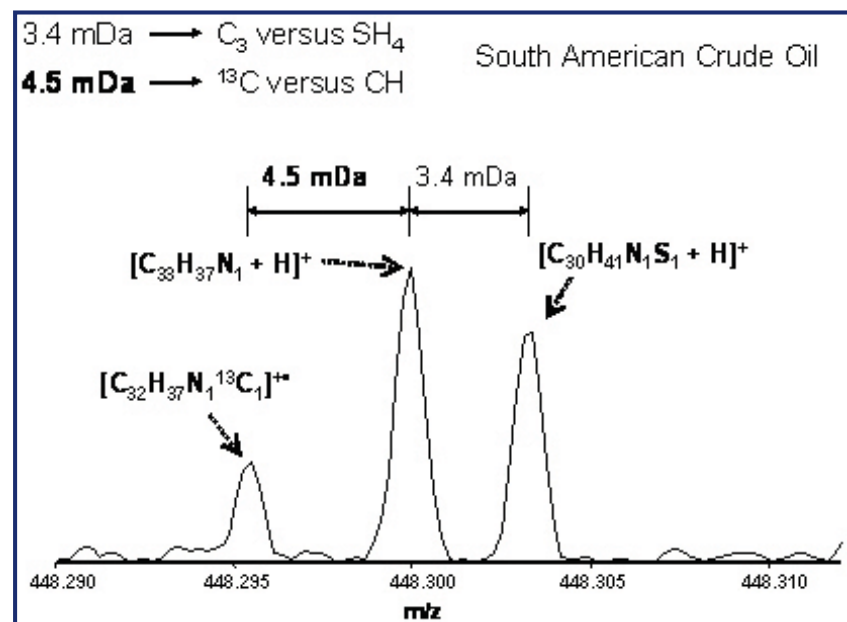
- This work was published in the *Journal of the American Society of Mass Spectrometry* (2007).

**MOLECULAR STRUCTURE FROM MOLECULAR MASS**

Jeremiah M. Purcell (NHMFL Tallahassee; FSU Chemistry & Biochemistry), Ryan P. Rodgers (NHMFL Tallahassee; FSU Chemistry & Biochemistry), Christopher L. Hendrickson (NHMFL Tallahassee; FSU Chemistry & Biochemistry), and Alan G. Marshall (NHMFL Tallahassee; FSU Chemistry & Biochemistry)

**RESULTS AND DISCUSSION**

The smallest chemically distinct unit of matter is a molecule. High-resolution mass spectrometry can determine the chemical formula of a molecule: i.e., its number and types of constituent atoms, e.g.,  $C_cH_hN_nO_oS_s$ . However, mass alone cannot usually determine how the atoms are linked together in the molecular structure. NHMFL/FSU researchers have recently shown that ultrahigh-resolution Fourier transform ion cyclotron resonance mass



spectrometry (FT-ICR MS) can differentiate molecules containing a nitrogen atom in a five-member vs. six-member aromatic ring (as in crude oil). Atmospheric pressure photoionization distinguishes the two kinds of rings in a single positive-ion mass spectrum (a five-member ring yields  $M^+$  ions, whereas a six-member ring yields  $(M+H)^+$  ions)<sup>1</sup>. High magnetic field FT-ICR MS is required, because it is necessary to resolve molecules differing in mass by less than 0.005 of the mass of the smallest atom (hydrogen)—see Figure.

**ACKNOWLEDGEMENTS**

This work was supported by the NSF National High-Field FT-ICR Mass Spectrometry Facility (DMR 06-54118), Florida State U., and NHMFL.

**REFERENCES**

- [1]. Purcell, J. M. *et al.*, *J. Am. Soc. Mass Spectrom.* **18**, 1265-1273 (2007).

This work pushes bulk-prepared  $MgB_2$  to new limits, using ball milling as a means both to mix C into  $MgB_2$  and to greatly refine the grain size of the  $MgB_2$ . Even after hot isostatic sintering at 1000° C, it is possible to obtain grain sizes of 20 nm or less. The strong scattering produced by the C and fine grain size mainly enhance the properties in the inferior H parallel to the c axis direction, where it is most useful to applications. The irreversibility field has thus been enhanced from about 11 to 17 T while the very fine grains also benefit flux pinning, generating the highest critical current densities yet reported in bulk  $MgB_2$ .

- This work was published in *Superconductivity Science and Technology* (2008). Another paper published on this work in 2007, "Understanding the route to high critical current density in mechanically alloyed  $Mg(B_{1-x}Cx)_{10}$ " was chosen for inclusion in the 'Superconductor Science and Technology' (SuST) 2007 highlights.

**IMPROVING PERFORMANCE IN BULK MAGNESIUM DIBORIDE BY IMPROVED PROCESSING**

B.J. Senkowicz, J. Jiang, J. Zhou, P.J. Lee, E.E. Hellstrom, and D.C. Larbalestier (FSU-NHMFL Applied Superconductivity Center)

**INTRODUCTION**

Bulk form magnesium diboride ( $MgB_2$ ) is a promising material for use in constructing superconducting magnets with operation temperatures up to 20 K, or mid-field magnets (< 10 T) operating at 4.2 K. The processing conditions leading to optimal properties are the object of much investigation. In this work, we examined the effects of carbon alloying, high energy ball milling, and heat treatment temperature on performance (critical current density) and used our results to describe a complex interaction between processing parameters and properties focusing on electron scattering, grain size, lattice composition, and electrical connectivity.

**EXPERIMENTAL**

Three sample sets (pellets) were synthesized with varying carbon content by a process involving mechanical alloying (in high energy ball mill) of pre-reacted  $MgB_2$  powder with graphite powder (dopant), followed by hot isostatic pressing. Set A was unmilled and undoped. Set B was milled and undoped. Set C was both milled and doped. One sample from each set was HIP treated at 900°C, 950°C, 1000°C, 1150°C, and 1500°C. The sintered pellets were sectioned with a diamond saw, and their properties investigated. This experiment used the fabrication, characterization, and microscopy facilities located at the Applied Superconductivity Center, as well as the 33 T resistive magnet in the DC field user facility.

**RESULTS AND DISCUSSION**

We found that  $J_c(H,T)$  benefited strongly from fine grain sizes <50 nm, available by heat treating at 950°C or lower T. However, sintering was limited below 1000°C causing  $J_c$  to be limited by electrical connectivity. In this work we found that high energy ball milling reduced the T necessary to achieve ~50% of full connectivity from > 950°C to ~900°C in undoped samples. This advance enabled successful heat treatment at 900°C, resulting in an unprecedented combination of connectivity and fine grains Figure 1. When beneficial carbon was added to the material, we were able to achieve extremely high  $J_c$  (8 T, 4.2 K) >  $5 \times 10^4$  A/cm<sup>2</sup>. Further investigation revealed that the benefits of fine grain size are not limited to flux pinning improvement, but to changes in the electron scattering state of the material which result in improvement of the critically important performance-limiting  $H_{c2}(H//c\text{-axis})$  with no significant change to  $H_{c2}(H//ab\text{-plane})$ .

**CONCLUSIONS**

This work simultaneously explored several processing variables and resolved their interrelated effects, resulting in excellent material performance and the knowledge necessary to tailor performance to the temperature and magnetic fields of applications by manipulating heat treatment schedules, mechano-chemical processing, and composition.

**ACKNOWLEDGEMENTS**

This work was financially supported by the US Department of Energy through the Division of High Energy Physics (DE-FG02-07ER41451) and Office of Fusion Energy Science (DE-FG02-06ER54881) and also our NSF focused research group DMR-0514592.

**REFERENCES**

- [1] Senkowicz, B.J., *et al.*, *Superconductor Sci. Technol.* **20**, 650-657 (2007).  
 [2] Senkowicz, B.J., BJ; Mungall, RJ; Zhu, Y, *et al.* *Superconductor Sci. Technol.* **21** (2008)

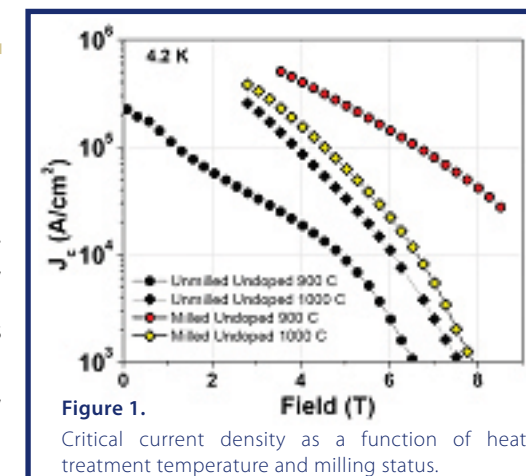


Figure 1. Critical current density as a function of heat treatment temperature and milling status.

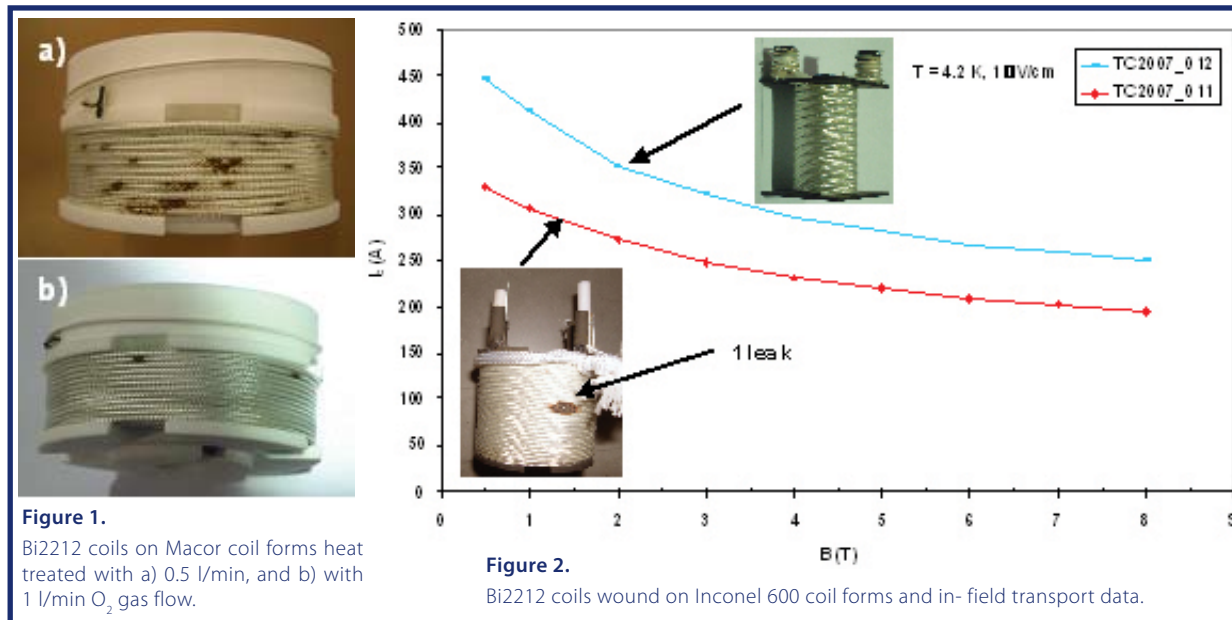


Round wire Bi-2212 coil technology emerged during 2007 with a series of 12 coils in which many of the obstacles to immediate exploitation of the promise of Bi-2212 were identified. Along the path to a 7 Tesla insert coil aimed at surpassing the previous Bi-2212 coil record of 5T in a 20T background, the potential of RW Bi-2212 is now established. The tendency of the conductor to leak in the presence of the useful and widely used structural ceramic (Macor) means reliance on more complex insulations, as does the tendency to react with braided mullite insulations. Identification of these issues has led to better performance with all-metal coil forms such as Inconel 600. Extensive conductor evaluation has shown the need to sharpen the superconducting transition and to avoid degradation of the connectivity of the conductors by any step in the reaction process. This work lays out the key issues for making this new magnet technology viable.

## Bi2212 CONDUCTOR AND COIL TECHNOLOGY FOR HIGH FIELD MAGNETS

**U.P. Trociewitz, Y. Jiang, E.E. Hellstrom, W.D. Markiewicz, J. Schwartz, and D.C. Larbalestier (Applied Superconductivity Center); S. Hong, Y. Huang, H. Miao, M. Meinesz, B. Czabaj (Oxford Superconducting Technology Inc., NJ); I.H. Mutlu (Harran Üniversitesi, Turkey)**

Development of  $\text{Bi}_2\text{Sr}_2\text{CaCu}_2\text{O}_{8+x}$  (Bi2212) conductor for high-field magnet technology applications is a focus at the Applied Superconductivity Center (ASC)<sup>1</sup>. A design of a high field insert magnet manufactured using Bi2212 round wire in a wind and react (W&R) approach has been developed. In its current configuration the magnet will deliver 7 T in a background magnetic field of 18 T. The magnet design consists of four sub-shells with varying amount of external reinforcement on each shell and will have a bore size of 30 mm. The wire is Bi2212/Ag-alloy, 85 x 7 multifilament wire manufactured by Oxford Superconducting Technology (OST). It has a total diameter of 1.3 mm including a 0.15 mm thick  $3\text{Al}_2\text{O}_3\text{-}2\text{SiO}_2$  mullite fiber braid<sup>2</sup>. To understand and



solve potential issues with thermo-processing of larger winding packs and other basic technology issues, a series of small sample-coils have been wound on mandrels made from Macor, a machinable glass-ceramic. They were heat-treated and studied regarding superconducting, and microstructural properties, as well as regarding chemical compatibility between conductor, electrical insulation and structural materials. The coils were heat-treated applying the typical three-step heat-treatment process in flowing  $\text{O}_2$  including partial-melt, recrystallization, phase formation and phase refinery steps. Incompatibility issues were evident between the conductor, insulation braid and Macor. With all coils wound on Macor mandrels excessive leakage was found that could only be partially alleviated by changing heat treatment parameters and increase of gas flow, as shown in Figure 1. Scanning electron microscopy (SEM) and energy dispersive spectroscopy (EDS) revealed that Macor decomposes as it reacts with the conductor releasing Mg and F. It also revealed reactions between the conductor and the insulation braid causing erosion of the Ag-alloy sheath and transformation of the mullite into a brittle glass that may also reduce  $\text{O}_2$  diffusion into the conductor that is needed to complete Bi2212

phase formation. After replacing Macor coil forms with Inconel 600 coil forms leakage almost disappeared, as seen in Figure 2. This indicates that chemical reactions play a much stronger role in the cause of conductor leakage than other potential reasons that have been suggested previously like pre-existing defects, pin-holes, or internal pressure build up caused by the formation of  $\text{CO}_2$  inside of the conductor. Comparison of transport data of short samples and coils show that though the conductor suffers from connectivity issues it is possible to manufacture W&R coils with decent performance. To increase packing density and hence the engineering critical current density, alternatives to the mullite braid insulation are being considered. Sol-gel coating with  $\text{ZrO}_2$  has shown promising results in short samples and needs to be evaluated further.

### REFERENCES

- [1] Weijers, H.W., Trociewitz, U.P., Marken, K., Meinesz, M., Miao, H., Schwartz, J., *Supercond. Sci. Technol.* **17** (2004) 636-644.  
 [2] Miao H, Marken K R, Meinesz M, Czabaj B, Hong S, Twin A, Noonan P, Trociewitz U P, Schwartz J, *IEEE Trans. Appl. Supercond.* **17**(2) (2007) 2262 – 2265.

Work toward a conical bore high field magnet suitable for neutron scattering experiments made a significant advance with the test of the conical model coil. Here is an example of the further development of a core technology of the NHMFL allowing resistive magnets in new coil configurations, extending the range of magnet applications. The objective is to supply a conical magnet to the Spallation Neutron source (SNS) and thereby use the expertise of the NHMFL to meet critical instrumentation requirements of collaborating institutions.

## THE DESIGN AND TEST OF THE CONICAL MODEL COIL

**J. Chen, M.D. Bird, J. Toth, J.W. O'Reilly, S. Bole, Y. L. Viouchkov (FSU, NHMFL MS&T)**

### INTRODUCTION

In the autumn of 2006 a grant was awarded by the NSF for a Conceptual and Engineering Design (CED) of conical bore hybrid magnet suitable for neutron scattering experiments at the Spallation Neutron Source (SNS) in Oak Ridge, TN. The Conical Florida-Bitter (CFB) technology (pat. pend.) is the novel technology enabling for the design of this magnet. We have built a CFB model coil that has been tested to high current-density, power density, stress and field at the MagLab.

### THE DESIGN OF THE CONICAL MODEL COIL

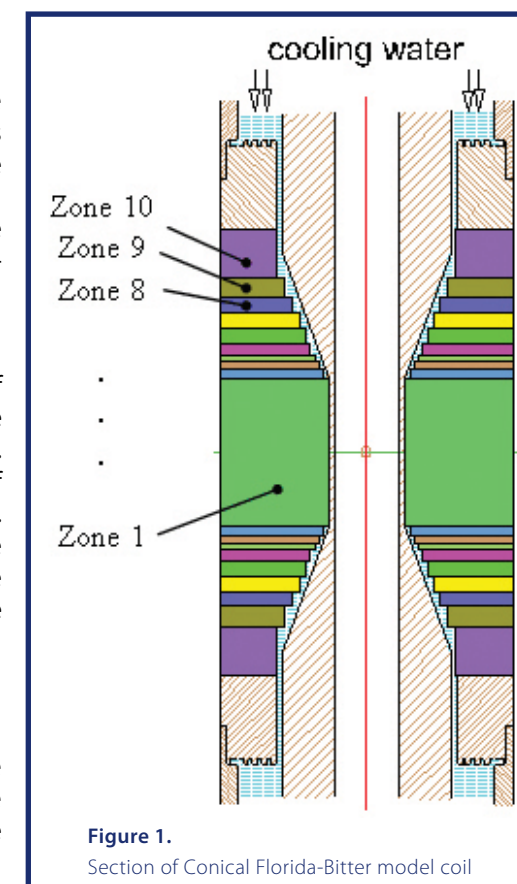
The basic design requirements include: 32mm bore, 15° half angle, 5mm sample diameter and dc power less than 8MW. The disks of a 30T magnet A coil are used to build the model coil. The unique feature in CFB technology is that the inner radii of the disks in different zones are different, as shown in Figure 1. Therefore the distribution of the current density, temperature and stresses are different for each zone and need to be calculated zone by zone. The main design parameters and the detailed zone parameters are listed in reference<sup>1</sup>.

### EXPERIMENTAL

The conical model coil was installed in the housing, which was especially designed for the testing of varied coils, and the whole assembly was inserted in the existing 20-T 200-mm bore resistive magnet (large bore in cell 4). Four different tests were carried out, including high power testing (insert only), high stress testing (insert + outsert), cyclic testing and destructive testing. Water temperature at three different positions (close to zone 2, zone 9 and coil outer radius respectively) was measured in order to evaluate cooling performance.

### RESULTS AND DISCUSSION

In general, the model coil worked very well. It generated 11.5 T at 15 kA and 14.1 T at 18 kA current. The power consumed was very close to the design value, implying that the cooling effect system performed as intended.



While designed for 15 kA, the coil worked at 18 kA current. In addition, the clamping force on the coil proved to be large enough to handle the electro-magnetic torque. The whole structure was very stable.

### CONCLUSIONS

The design of the conical model coil is complete. It was reviewed by an international committee in November 2007. The model coil was tested in Dec. 20, 2007. It generated 14.1 T in a background field of 19.4T for a total of 33.5 T. The CFB technology, therefore, is proved to be suitable for the high-field neutron and photon scattering experiments. It will enable such experiments at higher fields than presently available.

### REFERENCES

[1] Bird, M.D., *et al.* submitted to IEEE applied superconductor, 2007

An essential step forward for ultra-high field NMR or MRI is the development of instrumentation that allows for the optimization of magnetic field homogeneity in high-field resistive and hybrid magnets. The challenge is to develop shims that can be adjusted to provide corrections throughout a large range of available background field enabling scientific users to study the field dependence of various scientific phenomena such as nuclear magnetic relaxation. With the goal in mind of obtaining a target of  $1 \times 10^{-6}$  field homogeneity in the future 36T Series-Connected Hybrid magnet system, Mag Lab scientists have developed a novel shimming technique that locates resistive shims on the inner bore of the resistive magnet to allow cooling of the shims from the pre-existing resistive-magnet cooling water supply. A complete working shim set has been built and will be installed in the 25 T Keck Magnet in 2008. The 25 T Keck Magnet will serve as a staging area for the development of shims to be used in the 36T Series-Connected Hybrid.

• *This work has been accepted for publication in IEEE Transactions of Applied Superconductivity.*

## RESISTIVE SHIMS FOR HIGH-FIELD RESISTIVE AND HYBRID MAGNETS

T. A. Painter, M. D. Bird, S. T. Bole, A. J. Trowell, K. K. Shetty, W. W. Brey (NHMFL), Jingping Chen

### INTRODUCTION

The National High Magnetic Field Laboratory (NHMFL) has been funded by the National Science Foundation to construct a Series-Connected Hybrid (SCH) magnet system operated with a single 12 MW power supply which will produce 36 teslas and  $10^{-6}$  field homogeneity and stability over a 1 cm diameter spherical volume<sup>1</sup>. The NHMFL presently operates a 25 T resistive magnet, referred to as the Keck magnet, which employs ferroschims that correct the field homogeneity to  $1.2 \times 10^{-5}$  at 25 T over a 1 cm DSV<sup>2</sup>. The targeted SCH specification will extend the present boundary of the high-field, high-homogeneity experimental environment to  $10^{-6}$  homogeneity at 36 T. As a first demonstration, a new shimming technique will be installed and operated in the Keck magnet to improve its homogeneity from  $10^{-5}$  using ferroschims ( $10^{-4}$  unshimmed) to  $10^{-6}$  at 25 T. Resistive shims have been selected for the SCH due to their operational flexibility. Unlike ferroschims, resistive shims can be adjusted to provide corrections throughout the range of available background field enabling scientific users to study the field dependence of various scientific phenomena such as nuclear magnetic relaxation. The resistive shims can also be adjusted as needed to optimize the field correction as resistive magnet coils are replaced over the system lifetime.



Figure 1.

The Keck Shims were produced by Advanced Magnet Lab to demonstrate and characterize performance and operation in a 25 T resistive magnet before integrating into the NHMFL SCH.

### NOVEL SHIMMING TECHNIQUE

A novel shimming technique (patent application no. 60/854654) is proposed for the SCH that locates resistive shims on the inner bore of the resistive magnet to allow cooling of the shims from the pre-existing resistive-magnet cooling water supply. The novel technique employs single-turns capable of carrying 150 A as opposed to, for example, 150 turns at 1 amp to minimize the electrical insulation that impedes cooling from the water channel. The traditional conductor locations and circuits for the transverse shims have been modified to allow a single conductor in a novel circuitry for both the X and ZX (and Y and ZY) terms. The modified transverse shim circuits in combination with the optimized conductor axial location resulted in elimination of any lengthwise overlap and the associated increase in thermal impedance. In addition, a Z0 coil is fabricated into the shim set as part of the system to correct for temporal field instabilities in the magnetic field. The resultant radial build of the shim assembly is less than 5.0 mm – a key parameter at the inner bore of a high-field magnet. As an important developmental step, a fully operational shim set will be installed in the Keck magnet to allow the system to be demonstrated and characterized by regular user operation before being employed in the SCH.

### CONCLUSIONS

A novel shimming technique has been conceptualized, designed and built (Figure 1) for correcting spatial inhomogeneities inside a high-field resistive or hybrid magnet system. The shimming technique uses resistive conductors located on the bore tube of the resistive magnet where (a) they can be cooled by a pre-existing flow of water required for the resistive magnet and (b) they require several orders of magnitude less ampere turns than superconducting shims traditionally located on the outer diameter of the superconducting magnet. A novel shim circuitry has been employed which allows the transverse shim terms to be divided and recombined to allow a minimum of turns. A complete working shim set with six terms has been built and will be installed in the 25 T Keck Magnet at the NHMFL in early 2008 to demonstrate the feasibility of this technique to meet the targeted objective of the SCH of  $1 \times 10^{-6}$  homogeneity in a 36 T central field region.

### ACKNOWLEDGEMENTS

Many thanks to Rainer Meinke and Gerry Stelzer at Advanced Magnet Lab, Inc., Melbourne, FL ([www.magnetlab.com](http://www.magnetlab.com)) for the invaluable contributions regarding the fabrication processes for this resistive shimming technique.

### REFERENCES

[1] Miller, J.R., *et al.*, *IEEE Trans. Appl. Supercond.*, **14** (2), 1283-1286 (2004).  
[2] Bird, M., *et al.*, *IEEE Trans. Appl. Supercond.*, **12** (1), 447-451 (2002).

Angular dependent resistivity measurements of  $\text{YBa}_2\text{Cu}_3\text{O}_7$  (YBCO) films, in pulsed magnetic fields (H) up to 50T, have settled a long-standing debate on the presence of a smectic phase in “lower anisotropy” high  $T_c$  superconductors. When H is aligned with the Cu-O layers, the rapid increase of the vortex melting line at low temperatures together with the critical exponent values, confirm the presence of a liquid-smectic transition. Also, up to 50T, correlated defects strongly reduce the motion of vortices well into the liquid phase.

• *This work was published in Physical Review Letters (2008) and was supported by the Magnet Lab's User Collaboration Grants Program*

## ANGULAR DEPENDENCE OF THE MELTING LINE OF $\text{YBa}_2\text{Cu}_3\text{O}_7 + \text{BaZrO}_3$ THIN FILMS

S. A. Baily, B. Maierov (NHMFL/STC, LANL); F. F. Balakirev, M. Jaime (NHMFL, LANL); H. Zhou, S. R. Foltyn, L. Civale (STC, LANL)

### INTRODUCTION

Deep inside the superconducting state when a magnetic field penetrates a superconductor, vortex matter can exist in solid or liquid phases. The nature of these phases is given by the nature of the pinning centers present.<sup>1</sup> Pinning centers make high temperature superconductors (HTS) useful by stabilizing the solid phase and enabling films to carry current without dissipation. When the magnetic field or temperature increases, the solid vortex lattice melts and electrical resistance increases. The most interesting case occurs when field is aligned with the copper oxide planes of HTS and many types of pinning centers are present.



**EXPERIMENTAL**

Electrical ac-transport was used to measure the vortex dissipation in the liquid phase as well as to determine the melting line (where dissipation goes to zero), as a function of angle for  $\text{YBa}_2\text{Cu}_3\text{O}_7$  (YBCO) films in the 50 T short-pulse magnet using the newly rebuilt rotator probe. The effect of naturally grown defects on the melting line was studied.

**RESULTS AND DISCUSSION**

We find that near 80 K ( $H > 40\text{T}$ ), when the magnetic field is aligned with the layers, the melting line turns upward and the critical exponent that describes the rise in resistivity upon entering the liquid state becomes similar to that of a liquid crystal melting transition as predicted for layered superconductors.<sup>2</sup> Also, we observe that up to the highest field measured (50 T) correlated defects arrest the motion of vortices well into the liquid phase. At intermediate angles, the complete vortex dissipation can be scaled using the mass anisotropy model.

**CONCLUSION**

A long-standing debate about the existence of a smectic vortex phase in "low anisotropy" HTS has been settled, with evidence for a smectic vortex phase in optimally doped YBCO at fields higher than 40 T.<sup>3</sup>

**ACKNOWLEDGEMENTS**

This work was supported by the NSF through the NHMFL and NHMFL UCGP, the State of Florida and the DOE.

**REFERENCES**

[1] G. Blatter, *et al.*, *Rev. Mod. Phys.* **66**, 1125 (1994).

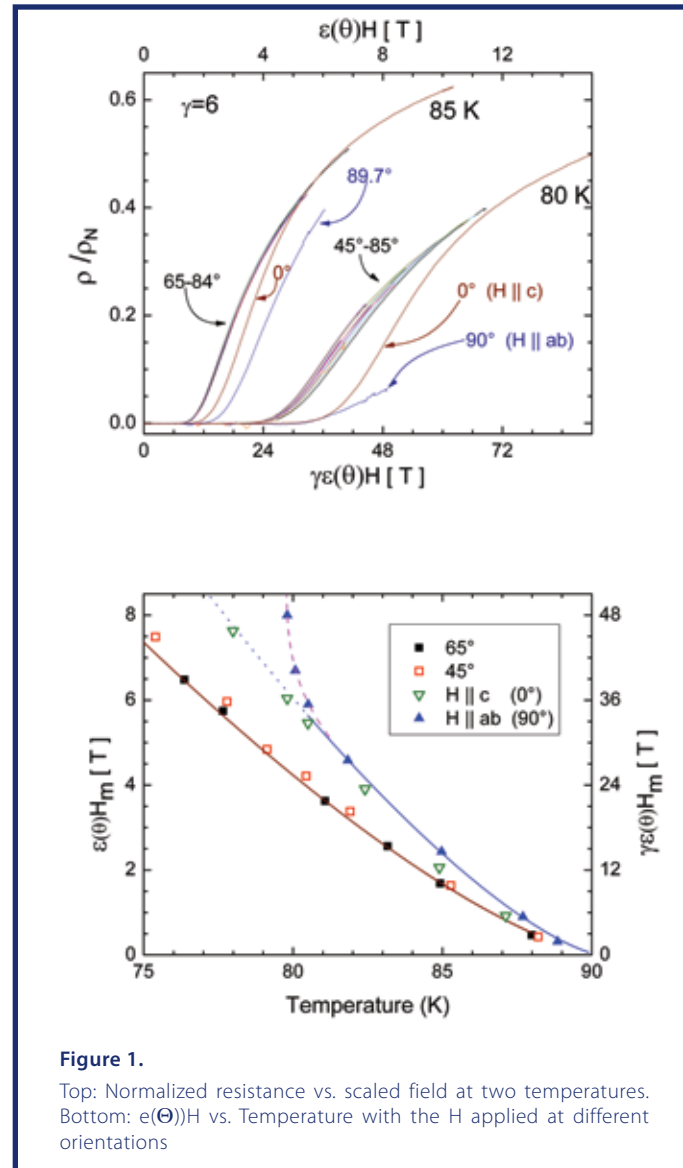


**Figure 1.**  
Top: Normalized resistance vs. scaled field at two temperatures. Bottom:  $\epsilon(\Theta)H_m$  vs. Temperature with the H applied at different orientations

In spite of the vital advantages of round wire for magnet use, the emerging 2nd generation HTS wire using YBCO tapes is proving very attractive for applications. Thieme *et al.* present data on tapes made by the AMSC RaBITS technique in a form useful for very high field solenoid use. Current densities of almost 500 A/mm<sup>2</sup> at 25 T make it clear that these materials are going to be very attractive for high field solenoids.

**HIGH FIELD STABILITY EXPLORATION OF SECOND GENERATION HTS**

C.L.H. Thieme, K. Gagnon, (American Superconductor - AMSC), Honghai Song, J. Schwartz (NHMFL/FSU)

**INTRODUCTION**

2G HTS wire is based on high performance thin film YBCO superconductor. AMSC uses a bi-axially textured substrate with a thin epitaxial oxide buffer layer (RaBITS™). The YBCO layer is grown using a solution-based coating process carried out on a 4 cm wide web. After completion of all coatings the conductor is slit to multiple 4 mm widths. These are laminated on both sides to a 4.4 mm copper foil<sup>1</sup>, resulting in a so-called 344 superconductor. For ac applications a stainless laminate can be selected<sup>2</sup>.  $I_c$  improvements are obtained through improved chemistry and reactor conditions<sup>3</sup>.

The main objective of this STTR Project is the exploration of the suitability of Second Generation HTS for high heat load, high radiation environment applications. The Phase I aimed at an extensive characterization of  $J_c(B, T, \Theta)$  (where  $\Theta$  is the angle between the field and surface of the conductor) and establishing the thermal limit in various stability experiments using small coils. The operating regime of interest is low temperatures (4.2-27 K) and fields up to 25 T. Previous measurements at the NHMFL demonstrated an engineering critical current of 225 A/mm<sup>2</sup> at 25 T, parallel field. We characterized short lengths of a new, thicker film conductor at 4.2 K and fields between 3 and 25 T. We then continued with the characterization of multiple 10m lengths. These were used to build various instrumental pancake coils, see Figure 1, intended for stability measurement at 4.2 k and fields of 6-7 T.

**EXPERIMENTAL**

The 344 superconductor for this STTR Project was made using a so-called double layer geometry, resulting in a 1.4  $\mu\text{m}$  thick YBCO layer with different pinning characteristics for top and bottom layer. The 4.4x0.2 mm conductor (0.88 mm<sup>2</sup> area) has 50% copper stabilizer. The conductor showed a critical current exceeding 100 A at 77 K, SF. Lengths of this conductor were used for measurements at high magnetic field, with field orientations parallel and perpendicular to the face of the tape-like conductor. In parallel fields the conductor was measured using an adapted ITER probe. Two pair of voltage taps were placed at 40 and 60 cm distance, with a minimum distance of 15-20 cm between current leads and outer voltage taps. The sample was always under compression. This worked well except for very high fields (24-25 T) when the conductor could buckle.



**Figure 1.**  
Epoxy impregnated pancake coil made of YBCO coated conductor. The coil is heavily instrumented for upcoming stability testing.

**RESULTS AND DISCUSSION**

In parallel fields the  $I_c$  reduction with field was gradual, as anticipated from earlier work. At 10, 15, 20 and 25 tesla the critical current was 643, 557, 486 and 418 A (or 1600, 1390, 1215 and 1045 A/cm-width), resulting in an overall critical current  $J_c$  (including copper stabilizer) of 670, 580, 506, and 435 A/mm<sup>2</sup>. These values are roughly proportional to the layer thickness compared to earlier values in 0.8  $\mu\text{m}$  thick YBCO films. In a perpendicular field the critical currents were much lower, again as expected based on earlier measurements, with  $J_c$  values of 208 (5 T), 133 (10 T), 101 (15 T), 83 (20 T) and 73 A/mm<sup>2</sup> (25 T). These values too were in line with what could be expected for the increased film thickness.

**CONCLUSIONS**

The high demonstrated engineering critical currents (475 A/mm<sup>2</sup> at 25 T) are of interest for those high field applications in which the HTS magnet section is placed in a background field with field parallel to the conductor. The measurements are the first and a good start in a series for a full characterization, before small pancake coils made of the same conductor will be tested for stability in a magnetic field.

**ACKNOWLEDGEMENTS**

This STTR Program is supported by the U.S. Department of Energy, Office of High Energy Physics.

**REFERENCES**

- [1] M.W. Rupich, U. Schoop, D.T. Verebelyi, C.L.H. Thieme, X. Li, W. Zhang, T. Kodenkandath, Y. Huang, E. Siegal, D. Buczek, W. Carter, N. Nguyen, S. Fleshler, J. Lynch, R. Harnois, "Development of Second Generation HTS Wire at American Superconductor", IEEE Trans. on Appl. Supercond. **17**, 3379 (2007).  
 [2] Li X et al, 2007 IEEE Trans. on Appl. Supercond. **17**, 3553 (2007).  
 [3] C.L.H. Thieme, K. Gagnon, J. Voccio, D. Aized, and J. Claassen, "AC application of Second Generation HTS wire", J Physics: Conf. ser. (JPCS), European Conference on Applied Superconductivity, September 2007, Brussels.

Controlling fusion energy, the source that drives the sun, is the objective of ITER, the International Thermonuclear Experimental Reactor. The NHMFL provides unique facilities for the testing of Nb<sub>3</sub>Sn superconductor intended for use in the ITER machine. In earlier work, the very large degradation of critical current with bending strain in advanced high current density internal tin process conductors was revealed. These measurements are made on single strands in pure bending, and are therefore a fundamental aspect of the performance of cables under more complex load patterns. In the recent work reported here of an expanded study, the large degradation associated with high current density internal tin wires is confirmed, and compared with the much lower degradation characteristic of conventional bronze process wires. A clear tradeoff between available current density and strain sensitivity is shown. These measurements are essential in providing the information necessary to make design selections for the ITER conductors.

**BENDING EFFECT ON Nb<sub>3</sub>SN SUPERCONDUCTING WIRES**

**Makoto Takayasu, Luisa Chiesa, Joel H. Schultz, Joseph V. Minervini (Massachusetts Institute of Technology, Plasma Science and Fusion Center), and John R. Miller (Oak Ridge National Laboratory)**

**INTRODUCTION**

Bending effects on Nb<sub>3</sub>Sn wires have been investigated to understand the critical current degradation of large Nb<sub>3</sub>Sn superconducting cables, such as the ITER conductors. A variable-bending device has been constructed for characterizing the critical currents of Nb<sub>3</sub>Sn superconducting strand under pure bending without uniaxial tension or compression. This device has been successfully developed<sup>1</sup> and has been used to test several Nb<sub>3</sub>Sn wires: ITER TF US wires of Luvata and Oxford internal-tin wires, and other ITER related Nb<sub>3</sub>Sn wires (European EAS bronze and EM-LMI internal tin, and Japanese Furukawa bronze wires).

**EXPERIMENTAL**

Pure bending experiments for various Nb<sub>3</sub>Sn wires were performed with our pure-bending device using the 20 T, 195 mm Bitter magnet at NHMFL. Our bending test device allowed applying pure bending strains to a strand during test operation in liquid helium<sup>1</sup>. The strand samples were placed on a support beam plate made of Ti-6Al-4V that was deformed through a series of pure bending states. This device can apply a large range of bending, up to 0.8% of the nominal bending strain at the wire surface. The actual peak bending strain of the filaments in the wires was about 65% of the nominal bending strain values, depending on copper/noncopper fraction. The critical currents were measured at every 0.1% increment of bending up to 0.8%. Irreversible degradation of the critical current due to bending was measured by releasing bending after each 0.1% increment.

**RESULTS AND DISCUSSION**

We tested five different Nb<sub>3</sub>Sn wires which were developed by the ITER parties. Three were internal-tin wires of recently developed ITER TF US Oxford and Luvata wires and EU EM-LMI wire. Two of them were bronze wires of EU EAS and Japanese Furukawa designs. The critical currents degraded with increasing the bending strains. At 0.8% nominal bending strains the critical currents of the internal tin wires were degraded by 47% for Oxford wire, 40% for Luvata wire and 30% for EM-LMI wires. Higher current density wire such as the Oxford wire seems to degrade more than lower current density wires. On the other hand with the same 0.8% nominal bending, bronze wires made by Furukawa and EAS both degraded by only 10%. After 0.8% bending, Oxford and Luvata wires showed 13% and 1.3% irreversible permanent degradation of their initial critical current values, respectively. It is noted that some wires such as the Furukawa wire show small improvements of the critical currents with applied bending up to about 0.3%.



**Figure 1.**  
A pure bending device is shown in the figure. The superconducting strand is mounted on a support beam and a groove is placed on the neutral axis of the beam to produce pure bending effect on the strand.

**ACKNOWLEDGEMENTS**

This work was supported by the U.S. Department of Energy, Office of Fusion Energy Science under Grant Number: DE-FC02-93ER54186 and the US ITER Project Office.

**REFERENCES**

- [1] D.L. Harris, et al., "Pure bending strand test of high performance Nb<sub>3</sub>Sn wires," Adv. Cryo. Eng., **54**, Plenum, N.Y., 341-348, (2008).

Hall effect measurements in YBCO at 12% doping have been extended to high B up to 45 T. It is found that the Hall coefficient  $R_H$  is positive at high temperatures, but becomes strongly negative below  $\sim 70$  K ( $T_C = 67.5$  K). This is believed to reveal the presence of electron pockets in the Fermi surface, which would then give rise to the previously observed quantum oscillations at low temperatures. It is proposed that electron pockets arise from a reconstruction of the Fermi surface, but the mechanism remains unidentified.

• This work was published in *Nature* (2007).

**NEGATIVE HALL COEFFICIENT IN THE NORMAL STATE OF HOLE-DOPED CUPRATE SUPERCONDUCTORS**

**N. Doiron-Leyraud, D. LeBoeuf, J.-B. Bonnemaïson, L. Taillefer (Sherbrooke); C. Proust (LNCMP); R. Liang, D. Bonn, W. Hardy (UBC); L. Balicas (NHMFL)**

**INTRODUCTION**

Earlier this year, quantum oscillations in the Hall resistance of the cuprate superconductor YBa<sub>2</sub>Cu<sub>3</sub>O<sub>y</sub> (YBCO) at 10% doping were observed<sup>1</sup>, convincingly showing that there is a Fermi surface in underdoped cuprates. Yet, the large magnitude and negative sign of the Hall resistance remained a puzzling issue given that YBCO is a hole-doped material. To understand this problem, we carried out further high-field measurements of the Hall resistance of YBCO.

**EXPERIMENTAL**

The Hall and longitudinal resistances were measured using a 4-point lock-in method. The samples, grown at UBC, were detwinned chain-ordered YBCO platelets with dopings of 10 and 12%. Measurements were done in the 45 T hybrid magnet in Tallahassee during the week of March 26-30, 2007. The current was long the a-axis and the magnetic field along the c-axis.

**RESULTS AND DISCUSSION**

In the figure on the right we show the Hall coefficient  $R_H$  measured in YBCO at 12% doping as a function of magnetic field up to 45 T. We see that  $R_H$  is positive above 70 K, and strongly negative below. Strikingly, at 70 K  $R_H$  vanishes at all fields, showing that the sign change is field independent and occurs above the superconducting  $T_C$  of 67.5 K. While previous studies on cuprates (see, e.g.,<sup>2</sup>) limited to low field below 25 T attributed this sign change to a negative flux flow contribution, our high field data demonstrate that a negative  $R_H$  at low temperature is an intrinsic normal-state property. These results, obtained at the NHMFL, were published in *Nature* on 22 November 2007.<sup>3</sup>

**CONCLUSIONS**

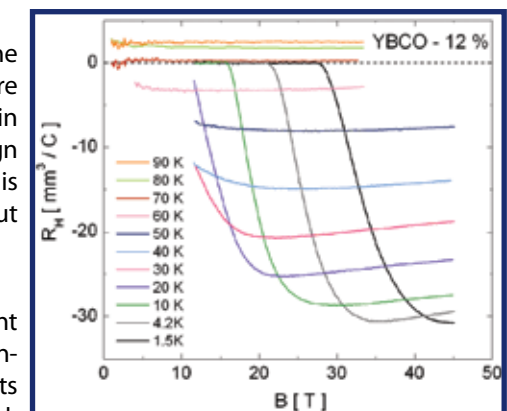
In order to understand the pronounced temperature dependence and sign change of  $R_H$ , one must invoke a scenario where two types of carriers - electrons and holes - with different mobilities are present. Because the quantum oscillations are observed at low temperature when  $R_H$  is negative, we conclude that they come from small electron pockets in the Fermi surface of YBCO. This observation can be explained by a reconstruction of the large cylindrical hole Fermi surface into small hole and electron pockets<sup>3</sup>, as is believed to occur in electron-doped cuprates because of antiferromagnetic ordering. The nature of the order causing the reconstruction in YBCO remains to be identified.

**ACKNOWLEDGEMENTS**

We acknowledge support from the Canadian Institute for Advanced Research, the NHMFL, and funding from the NSERC, the FQRNT, a Canada Research Chair, the NSF, and the State of Florida.

**REFERENCES**

- [1] Doiron-Leyraud, N. et al., *Nature* **447**, 565 (2007). [3] LeBoeuf, D., et al., *Nature* **450**, 533 (2007).  
 [2] Harris, J.M. et al., *Phys. Rev. Lett.* **71**, 1455 (1993).





Deviation from standard Fermi-liquid behavior is observed in the paramagnetic state of  $\text{Na}_x\text{CoO}_2$  at  $x = 0.75$ , and as a result of the interplay between itinerancy and localized  $S = 1/2$  moments on a triangular superlattice. The upturn in the low temperature specific heat and the anomalous scattering in the resistivity both point to the existence of a novel kind of low energy excitation. That these excitations appear to be suppressed by a magnetic field suggests that these are spin fluctuations. One suggestion is that the local moments form a spin liquid state which co-exists with itinerant electrons.

• This work is published in *Physical Review Letters* and was supported by the Magnet Lab's User Collaboration Grants Program.

## LOCAL MOMENT, ITINERANCY AND DEVIATION FROM FERMI LIQUID BEHAVIOR IN $\text{Na}_x\text{COO}_2$ FOR $0.71 \leq x \leq 0.84$

L. Balicas (NHMFL); Y. J. Jo (NHMFL); G. J. Shu (National Taiwan University); F. C. Chou (National Taiwan University); P. A. Lee (Physics-MIT)

### INTRODUCTION

We report the observation of Fermi surface (FS) pockets via the Shubnikov de Haas (SdH) effect in  $\text{Na}_x\text{CoO}_2$  for  $x = 0.71$  and  $0.84$ , respectively<sup>1</sup>. Our observations indicate that the FS expected for each compound intersects their corresponding Brillouin zones, as defined by the previously reported superlattice structures<sup>1</sup>, leading to small reconstructed FS pockets, but only if a precise number of holes per unit cell is localized. For  $0.71 \leq x < 0.75$  the coexistence of itinerant carriers and localized  $S = 1/2$  spins on a paramagnetic triangular superlattice leads at low temperatures to the observation of a deviation from standard Fermi-liquid behavior in the electrical transport and heat capacity properties, suggesting the formation of some kind of quantum spin-liquid ground state.

### EXPERIMENTAL

We performed electrical transport measurements in  $\text{Na}_{0.71}\text{CoO}_2$  and  $\text{Na}_{0.84}\text{CoO}_2$  using the hybrid magnet in conjunction with a <sup>3</sup>He refrigerator and a rotating sample holder in order to detect Shubnikov de Haas oscillations. Results for  $x = 0.71$  are shown in Figure 1. While Heat capacity and resistivity measurements at low fields were performed by using a PPMS (Figure 2).

### RESULTS AND DISCUSSION

The SdH oscillations can only be understood by the intersection of the original Fermi surface of these materials with the superlattice induced Brillouin zone, if for both concentrations at least one hole per superlattice unit cell is localized. Thus for  $x = 0.71$  one has 2.5 itinerant holes coexisting with a localized moment per each 12 cobalts within the superlattice unit cell and 1 itinerant holes and one localized moment per 13 cobalts within the superlattice unit cell.

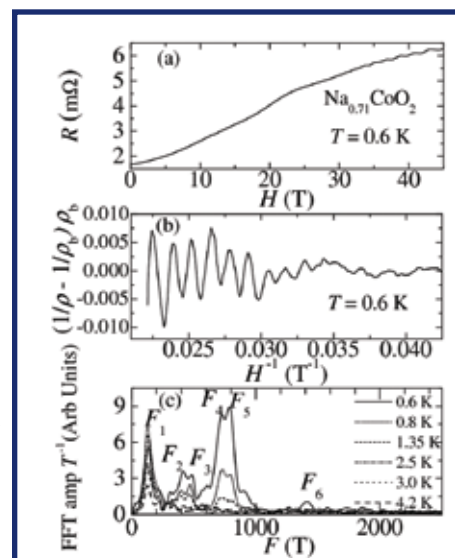


**Figure 1.** (a) Resistance  $R$  as a function of field  $H$  for a  $\text{Na}_{0.71}\text{CoO}_2$  single crystal at  $T = 0.6$  K. (b) The SdH effect or the oscillatory component of  $R$  in (a) as a function of  $H^{-1}$ . (c) Amplitude of the fast Fourier transform normalized by temperature  $T$  for several values of  $T$ . At least six frequencies are detected:  $F_1 = 125$  T,  $F_2 = 400$  T,  $F_3 = 475$  T,  $F_4 = 725$  T,  $F_5 = 800$  T, and  $F_6 = 1413$  T.

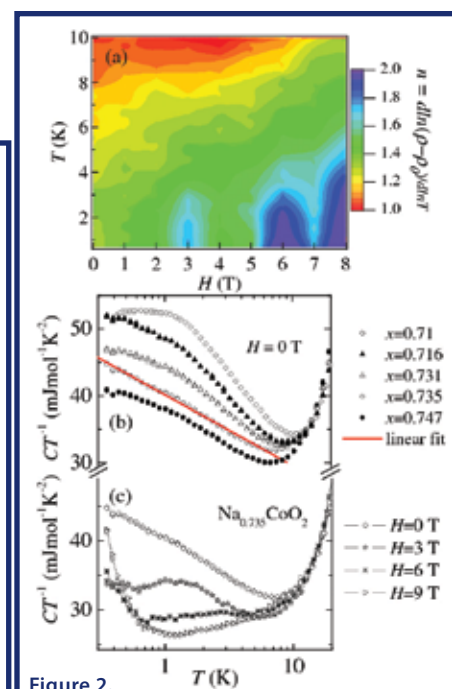


**Figure 2.** (a) The evolution of the exponent of the resistivity as a function of field  $H$  for a  $\text{Na}_{0.735}\text{CoO}_2$  single crystal. (b) Heat capacity normalized by temperature  $C/T$  as a function of  $T$  for several Na concentrations  $x$  in a semi-log scale. Straight line represents a linear fit to the  $x = 0.735$  data over the temperature range  $0.35 \leq T \leq 7$  K. (c)  $C/T$  as a function of  $T$  for  $x = 0.735$  and for several values of the field  $H$ .

### CONCLUSIONS

In summary, deviation from standard Fermi-liquid behavior is observed in the paramagnetic state of  $\text{Na}_x\text{CoO}_2$  as  $x = 0.75$ , and as a result of the interplay between itinerancy and localized  $S = 1/2$  moments on a triangular superlattice. The upturn in the low temperature specific heat and the anomalous scattering in the resistivity both point to the existence of a novel kind of low energy excitations. That these excitations appear to be suppressed by a magnetic field suggests that these are spin fluctuations. One suggestion<sup>1</sup> is that the local moments form a spin liquid state which co-exists with itinerant electrons. While our data does not allow us to draw any firm conclusion on the origin of the anomalous behavior, it is clear that the cobaltates offer a new window into possible novel ground states in a system with coupled local moments and itinerancy.

### ACKNOWLEDGEMENTS

LB acknowledges support from the NHMFL in-house research program, and YJJ from the Schuller fellow program.

### REFERENCES

- [1] Local moment, itinerancy and deviation from Fermi liquid behavior in  $\text{Na}_x\text{CoO}_2$  for  $0.71 \leq x \leq 0.84$ . Balicas, Y. J. Jo, G. J. Shu, F. C. Chou, and P. A. Lee, *Phys. Rev. Lett.* **100**, 126405 (2008).  
 [2] Woei Wu Pai, *et al*, *Phys. Rev. Lett.* **100**, 206404 (2008).

The properties of graphene, a single atomic sheet of graphite, are currently a subject of intense research. Much of the interest in this truly two-dimensional (2D) system stems from its unusual, linear low-energy dispersion relation, where the low-energy electronic excitations are described in terms of massless, chiral, Dirac fermions. This particular dispersion is thus expected to give rise to many properties that are different from those exhibited by other 2D systems. The report by Z. Jiang *et al.* describes several interesting phenomena that are observed when graphene is subjected to high magnetic fields. They include the observation of the integer quantum Hall (QH) effect at room temperature and of the new QH phases at low temperatures. Furthermore, a cyclotron resonance (CR) study of both single and bilayer graphene reveals several departures from the conventional CR on 2D semiconductor heterostructures. Some of the differences are attributed to the interactions between Dirac quasiparticles.

• This research has been published in *Science* **315**, 1379 (2007), and *Physical Review Letters*: **98**, 197403 (2007); **99**, 106802 (2007); **100**, 087403 (2008).

## LANDAU LEVEL SPECTROSCOPY OF GRAPHENE

Z. Jiang (Columbia University & NHMFL); E.A. Henriksen (Columbia University); K.I. Bolotin (Columbia University); Y. Zhang (Columbia University); L.-C. Tung (NHMFL); M.E. Schwartz (Columbia University); M. Takita (Barnard College); M.Y. Han (Columbia University); Y.-J. Wang (NHMFL); G.S. Boebinger (NHMFL); P. Kim (Columbia University), and H.L. Stormer (Columbia University & Bell Labs)

### INTRODUCTION

Graphene, a single atomic sheet of graphite, is a monolayer of carbon atoms arranged in a hexagonal lattice. The unique electronic band structure of graphene exhibits an unusual *linear* low-energy dispersion relation, quite different from the parabolic bands common to all previous two-dimensional systems. Most interestingly, this dispersion results in the charge carriers that mimic relativistic, massless Dirac particles, leading to intriguing new phenomena. In particular, a very unusual half-integer quantum Hall effect and a non-zero Berry's phase have been discovered in graphene.

### EXPERIMENT AND RESULTS

The Quantum Hall effect (QHE) is one example of a quantum phenomenon that occurs on a truly macroscopic scale. The signature of QHE is the quantization plateaus in the Hall resistance ( $R_{xy}$ ) and a vanishing magnetoresistance ( $R_{xx}$ ) in a strong magnetic field. The QHE, exclusive to two-dimensional metals, has led to the establishment of a new metrological standard, the resistance quantum,  $h/e^2$ , that contains only fundamental constants. As with many other quantum phenomena, the observation of the QHE usually requires low temperatures (the previously reported highest temperature was 30 K). In graphene, however, we have observed a well-defined QHE at room temperature (see Figure 1.) owing to the unusual electronic band structure and the relativistic nature of the charge carriers of graphene<sup>1</sup>. In addition, we have observed new QH phases at filling factors  $\nu = 0, \pm 1$ , and  $\pm 4$  at low temperatures and in high magnetic fields (see Figure 2. for the  $\nu = \pm 1$  and  $-4$  state), arising from the lifting of the spin and sublattice degeneracies of graphene Landau levels (LL)<sup>2</sup>.

The phenomenon of cyclotron resonance (CR) results when incident infrared radiation is absorbed by the excitation of carriers between neighboring LLs, with the absorbed frequencies corresponding to the LL energy separation. Since the 1950s, CR has been a fundamental tool for the investigation

of semiconductor bandstructures, which generally exhibit resonance energies that are linear in the magnetic field. Recently, we have made the first measurements of LL transitions via infrared transmission measurements in both single (Figure 3a, Ref.<sup>3</sup>) and bilayer (Figure 3b, Ref.<sup>4</sup>) graphene samples, in magnetic fields up to  $B = 18$  T. We find that both systems present radical departures from the usual CR, exhibiting LL transition energies that are linear in  $\sqrt{B}$  for single layer graphene, and that for bilayers show a shift from a linear-in- $B$  dependence at low energies to linear-in- $\sqrt{B}$  at higher energies. In further departures from traditional CR, resonance energies in both systems show a dependence on the LL index, while in single layers we have also observed interband in addition to intraband transitions. Departures from the expected ratios of the transition energies are interpreted as indicating physics of interacting Dirac quasiparticles, beyond a simple single particle picture.

#### ACKNOWLEDGEMENTS

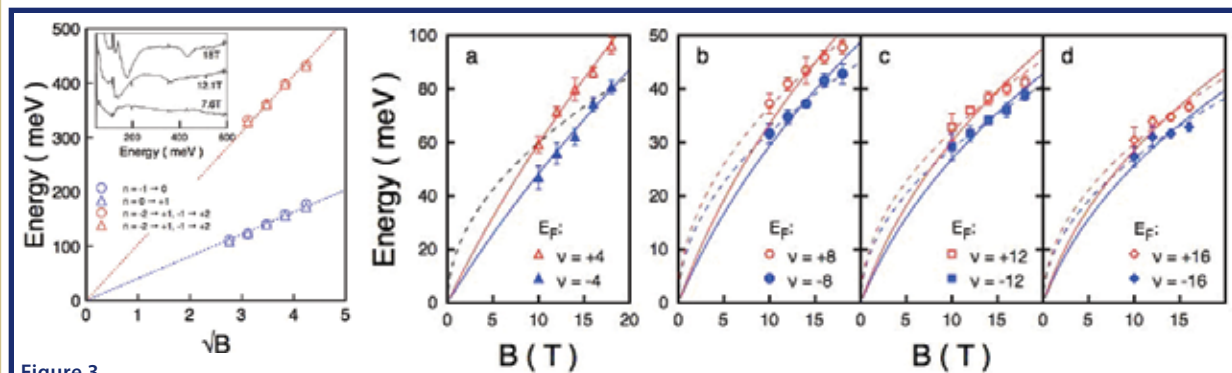


**Figure 3.** (left) LL transitions in single layer graphene. Inset shows normalized transmission for three B fields. Dashed lines are best fit to  $\sqrt{B}$ . (right) LL transitions among the first nine LLs in bilayer graphene. Dashed lines are fit to  $\sqrt{B}$ ; solid lines are fit to theory based on nearest-neighbor tight-binding approximation.

This work is supported by the DOE (DE-AIO2-04ER46133, DE-FG02-05ER46215 and DE-FG02-07ER46451), NSF (DMR-03-52738 and CHE-0117752), ONR (N000150610138), NYSTAR, the Keck Foundation, and the Microsoft Project Q.

#### REFERENCES

- [1] K.S. Novoselov, *et al.*, *Science* **315**, 1379 (2007).
- [2] Z. Jiang, *et al.*, *Phys. Rev. Lett.* **99**, 106802 (2007).
- [3] Z. Jiang, *et al.*, *Phys. Rev. Lett.* **98**, 197403 (2007).
- [4] E.A. Henriksen, *et al.*, *Phys. Rev. Lett.* **100**, 087403 (2008).

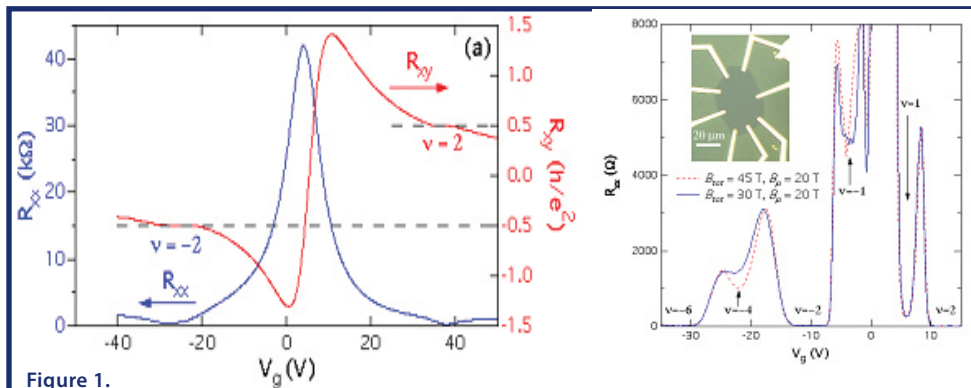


**Figure 1.** Magnetoresistance ( $R_{xx}$ ) and Hall resistance ( $R_{xy}$ ) as a function of the back gate voltage ( $V_g$ ) in a magnetic field of  $B = 45$  T at room temperature.

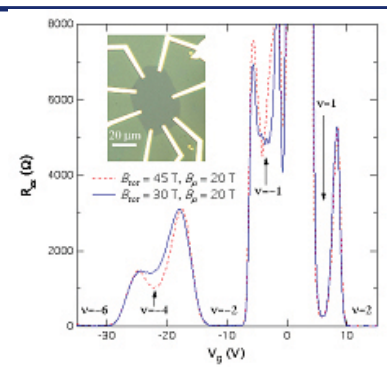


**Figure 2.**  $R_{xx}$  vs.  $V_g$  in tilted magnetic fields.

This describes a study of the thermoelectric response of clean Bi beyond the quantum limit to probe for high field anomalies. Accepted by *Science*, the authors observed new anomalies in the field dependence of the Nernst coefficient. These anomalies occur in the ultraquantum limit. They appear to be beyond the one-particle picture that successfully describes the low-field peaks associated with quantum oscillations and may constitute the first detected signatures of electron fractionalization in a bulk metal.

This work was published in *Science* (2007) and was supported by the Magnet Lab's Visiting Scientist Program.

## NERNST EFFECT IN ULTRAQUANTUM BISMUTH

Kamran Behnia (ESPCI-France), Luis Balicas (NHFML)

#### INTRODUCTION

The aim of this project was to study the thermoelectric response of a clean bulk metal beyond the quantum limit. A previous study detected giant quantum oscillations of the Nernst coefficient in elemental bismuth<sup>1</sup>. This experiment was set to probe any further anomaly at higher fields.

#### EXPERIMENTAL

We built a miniature probe to measure Nernst effect and used a He<sup>3</sup> refrigerator inside a resistive magnet yielding 33 T. Thermal conductivity in bismuth is field-independent. Therefore, a constant heat current yielded a constant temperature gradient along the sample. The signal-to-noise ratio in our DC voltage measurement was very satisfactory.

#### RESULTS AND DISCUSSION

We resolved three new anomalies in the field dependence of the Nernst coefficient beyond the quantum limit (see the figure). These anomalies occur in the ultraquantum limit. They appear to be beyond the one-particle picture that successfully describes the low-field peaks associated with quantum oscillations. They may constitute the first detected signatures of electron fractionalization in a bulk metal.

#### CONCLUSIONS

The results were published in *Science*.<sup>2</sup> We intend to pursue this investigation by studying the Nernst response of bismuth in the hybrid magnet up to 45 T next January.

#### ACKNOWLEDGEMENTS

KB is supported by DGA/D4S and ANR (ICENET project) and acknowledges a NHFML-VSP fellowship. LB is supported by the NHFML in-house research program.

#### REFERENCES

- [1] K. Behnia, M. -A. Méasson, Y. Kopelevich, *Phys. Rev. Lett.* **98**, 166602 (2007).
- [2] K. Behnia, L. Balicas, Y. Kopelevich, *Science* **317**, 1729 (2007)

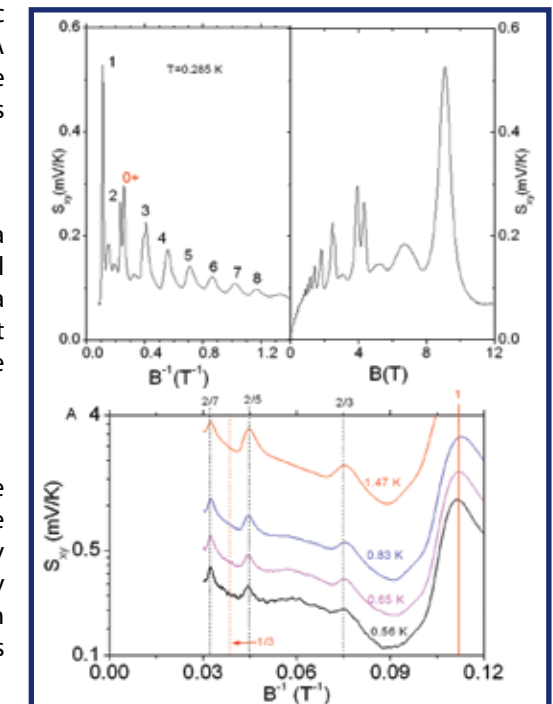


**Figure 1.** Nernst effect as a function of field below (upper panel) and above (lower panel) the quantum limit. Note the three additional peaks.



Among the reports of the Magnetism & Magnetic Materials category, there were a number of reports that present incremental inputs into further understanding of properties of the specific materials. Two particularly interesting reports were:

The report by J. Musfeldt *et al.*, where the phase diagram and ac magnetodielectric effect were studied in the frustrated Kagome lattice  $\text{Ni}_3\text{V}_2\text{O}_8$ .

- This work was published in *Physical Review B* (2007).

Also, the work of S. Hill, *et al.*, that describes the new technique to address the spin-dynamics in the so-called single-molecule magnet  $[\text{Mn}_{12}\text{O}_{12}(\text{CH}_3\text{COOH})_{16}(\text{H}_2\text{O})_4] \cdot 2\text{CH}_3\text{COOH} \cdot 4\text{H}_2\text{O}$ .

- This work was supported by the Magnet Lab's User Collaboration Grants Program and has been accepted by *Physical Review B*.

## CHEMICAL TUNING OF THE HIGH-ENERGY MAGNETO-DIELECTRIC EFFECT IN A FRUSTRATED KAGOME LATTICE MATERIAL

Musfeldt, J.L., Rai, R.C., Cao, J., Vergara, L.I., Brown, S. (Tennessee), Kasinathan, D. (Davis), Singh, D.J. (ORNL), Lawes, G. (Wayne State), Rogado, N., Cava, R.J. (Princeton), and McGill, S. (NHMFL)

### INTRODUCTION

Magnetic frustration and competing interactions in Kagome lattice materials give rise to complex magnetic field - temperature phase diagrams in the  $\text{M}_3\text{V}_2\text{O}_8$  system ( $\text{M} = \text{Ni}, \text{Co}, \text{Mn}$ ). In  $\text{Ni}_3\text{V}_2\text{O}_8$ , the low temperature incommensurate state displays both ferromagnetism and a finite polarization. One manifestation of magneto-electric coupling is a large static magneto-dielectric contrast. Sizable magneto-dielectric effects can also extend to relatively high energy in complex oxides due to spin-lattice-charge coupling. This work was done using a combination of optical spectroscopy, first principles calculations, and energy dependent magneto-optical measurements to elucidate the electronic structure and to study the phase diagram of  $\text{Ni}_3\text{V}_2\text{O}_8$ . The variable field work was carried out at the NHMFL.

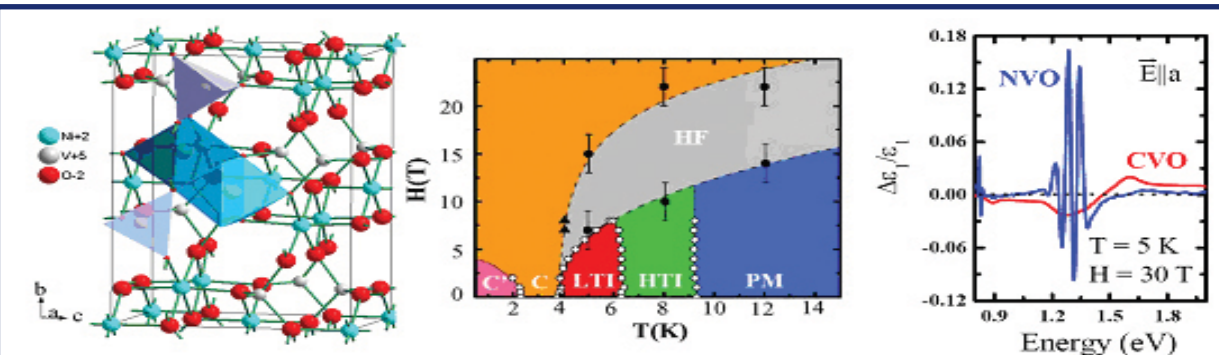


Figure 1. Crystal structure, H-T phase diagram, and high energy magneto-dielectric contrast for  $\text{Ni}_3\text{V}_2\text{O}_8$  compared with that of the Co analog, Refs. 1 and 2.

### RESULTS AND DISCUSSION

We recently discovered that sizable magneto-dielectric contrast can extend to relatively high energy in complex oxides. The effect can be positive or negative depending on the energy (Figure 1). In  $\text{Ni}_3\text{V}_2\text{O}_8$ , the intermediate gap, local moment character favors the observed field-induced modification of local structure and resulting high-energy dielectric contrast. Since ac magnetodielectric effect is a spectroscopic rather than capacitance measurement, dead layer contact and "leaky" magneto-resistance issues are avoided. Structure-property trends in the  $\text{M} = \text{Ni}, \text{Co}, \text{Mn}$  isostructural series are extremely interesting. The magneto-dielectric contrast is tunable depending on the chemical identity of the transition metal center (Figure 1), an effect that we attribute to a combination of lattice stiffness and hybridization effects. Complementary vibrational measurements on  $\text{Ni}_3\text{V}_2\text{O}_8$  single crystals reveal changes in magneto-elastic coupling between the nearly degenerate magnetic ground states and pinpoint the lattice displacements that are important for establishing the state with magneto-electric cross-coupling. A softer lattice in the Co analog compound works to reduce the high energy magneto-dielectric contrast (because the lattice relaxes at high temperatures and does not couple to the low temperature magnetic transitions) and remove the interesting magneto-electric phase from H-T phase space.

### ACKNOWLEDGEMENTS

We thank the U.S. Department of Energy for support of this work.

### REFERENCES

- Rai, R.C., *et al.*, *Phys. Rev. B*, **74**, 235101 (2006).
- Rai, R.C., *et al.*, *Phys. Rev. B*, **76**, 174414 (2007).

## PUMP-PROBE EPR STUDIES OF SPIN DYNAMICS IN SINGLE-MOLECULE MAGNETS

J. Lawrence, S. Hill (UF, Physics); F. Macia, J. Tejada (University of Barcelona, Physics); C. Lampropoulos, G. Christou (UF, Chemistry); P. V. Santos (Paul-Drude-Institut, Berlin, Germany)

### INTRODUCTION

We have developed a novel experimental technique that integrates high frequency surface acoustic waves (SAWs) with high frequency electron paramagnetic resonance (HF-EPR) spectroscopy ( $\sim 300\text{ GHz}$ ) in order to measure spin dynamics on fast time scales in single molecule magnets<sup>1</sup>.

### EXPERIMENTAL

A single crystal of  $[\text{Mn}_{12}\text{O}_{12}(\text{CH}_3\text{COOH})_{16}(\text{H}_2\text{O})_4] \cdot 2\text{CH}_3\text{COOH} \cdot 4\text{H}_2\text{O}$ , hereafter  $\text{Mn}_{12}\text{Ac}$ , was mounted on the surface of a piezoelectric  $\text{LiNbO}_3$  substrate containing interdigital transducers (IDTs) for the production of SAWs. After pumping the system out of equilibrium, by triggering magnetic avalanches with short SAW pulses, the evolution of the spin population within a fixed energy level is measured using HF-EPR spectroscopy in combination with fast data acquisition instrumentation. In addition to avalanche ignition, the SAWs can be used to perturb the system by merely heating it with a short pulse. The HF-EPR is simultaneously used as a probe of the time evolution of the spins as they relax back to equilibrium.

### RESULTS AND DISCUSSION

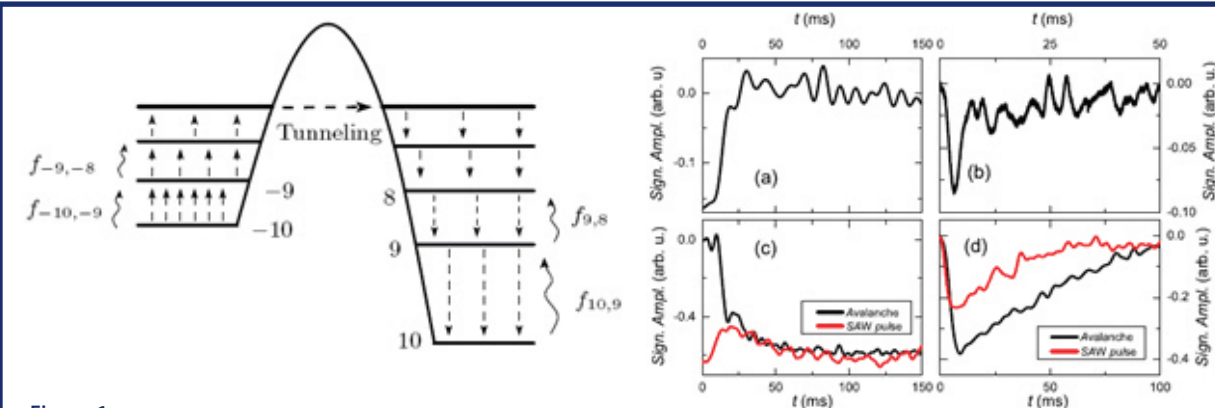


Figure 1. (left) Double potential well diagram for  $\text{Mn}_{12}\text{Ac}$  illustrating how spins relax during an avalanche. Spins in the right well relax to the ground state by emitting phonons, which result in heating of the system. This heating feeds back into the avalanche by exciting spins in the left well. (right) Evolution of the reflected microwave amplitude during an avalanche triggered via a SAW pulse. In (a),  $f = 270\text{ GHz}$ ,  $B = 1.1\text{ T}$  &  $m_s = -10$  to  $-9$ ; in (b),  $f = 237\text{ GHz}$ ,  $B = 0.58\text{ T}$  &  $m_s = -9$  to  $-8$ ; in (c)  $f = 320\text{ GHz}$ ,  $B = 0.54\text{ T}$  &  $m_s = 10$  to  $9$ ; and in (d),  $f = 268\text{ GHz}$ ,  $B = 0.54\text{ T}$  &  $m_s = 9$  to  $8$ . In (c) and (d), the red traces correspond to microwave absorption during a SAW pulse after the occurrence of the avalanche.

### CONCLUSIONS

Our results demonstrate how this new technique can be used to obtain energy resolved information about spin relaxation in single molecule magnets. In particular, we find that dynamics in the stable well are dominated by a phonon bottleneck effect, whereas the dynamics in the metastable well closely reflect the intrinsic spin-lattice driven magnetization dynamics.

### ACKNOWLEDGEMENTS

This work was supported by the National Science Foundation (grant nos. DMR0239481 and DMR0414809).

### REFERENCES

- Macia, F., *et al.*, *Phys. Rev. B*, **77**, 020403 (R)(2008).

The magnetoelectric coupling between a magnetic order and an electric polarization, (a type of magnetoelectric coupling), has never been observed before in organic materials. The necessary provision for the phenomenon is the loss of the center of inversion symmetry. In this report, the authors study the orthorhombic compound CDC ( $\text{CuCl}_2 \cdot 2(\text{CH}_3)_2\text{SO}$ ) in the antiferromagnetic state ( $T_N = 0.93$  K). The loss of the inversion symmetry is occurs at the spin-flop transition in a low magnetic field along the c-axis. It is the first example of coupled multiferrotic behavior in an organic material.

## FIELD-INDUCED FERROELECTRICITY IN AN ORGANIC QUANTUM MAGNET

V. S. Zapf (NHMFL - LANL), M. Kenzelmann (Paul Scherrer Institute, Zurich), F. Fabris (NHMFL - LANL), F. Balakirev (NHMFL - LANL), Y. Chen (NIST), C. Broholm (JHU)

### INTRODUCTION

Magnetoelectric coupling is generally rare and has never been observed before in an organic quantum magnet. The compound CDC ( $\text{CuCl}_2 \cdot 2(\text{CH}_3)_2\text{SO}$ ) however exhibits the necessary symmetry for certain applied magnetic fields  $H$  to allow an electric polarization  $P$  to coexist with antiferromagnetic (AFM) order. This compound contains chains of  $\text{Cu } S=1/2$  spins<sup>1</sup> that are weakly coupled via superexchange and exhibit AFM order below  $T_N = 0.93$  K, observed in specific heat and neutron diffraction measurements<sup>2</sup>. For  $H$  applied along the crystallographic a- and c-axes, the AFM order is suppressed, most probably due to a competition between interchain interactions and field-induced staggered fields<sup>2</sup>. For  $H$  along the orthorhombic c-axis, AFM order is suppressed by  $H \sim 4$  T (see Figure 1). A spin-flop transition above  $H_{sf} = 0.35$  T leads to a magnetically ordered state (AFM B) that breaks inversion symmetry along the b-axis for  $0.35 \text{ T} < H < 4$  T.

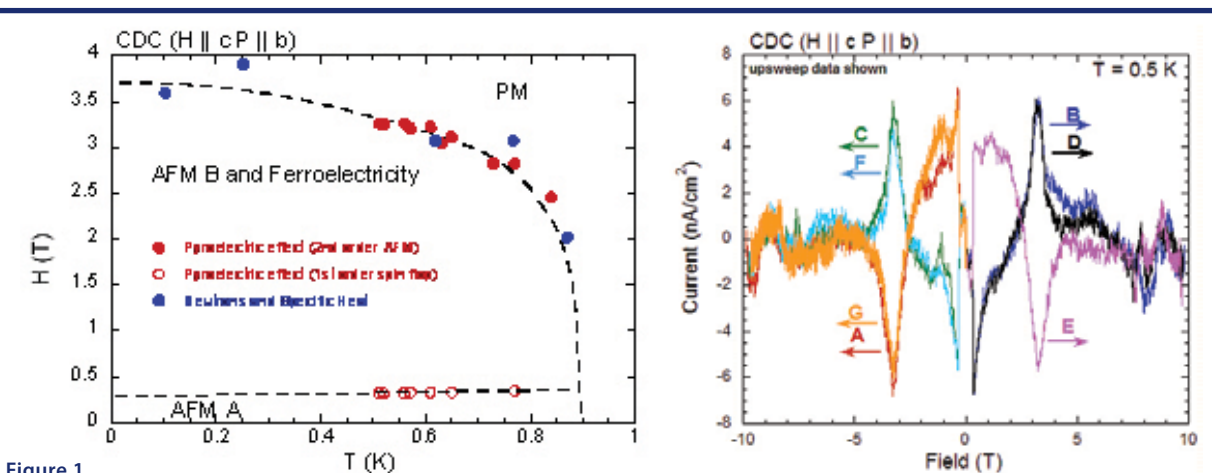


Figure 1.

Phase diagram of CDC showing regions of AFM with inversion symmetry (AFM A), AFM without inversion symmetry (AFM B) ferroelectric polarization, and paramagnetism (PM). Neutron and specific heat data is from Refs. 3,4.

Figure 2.

Magnetoelectric current measured on the upswing of a 50 T short pulse magnet. Consecutive pulses A – F are shown, where the sign of  $P$  depends on whether the field sweep is in the same or opposite direction as the previous sweep.

### EXPERIMENTAL

We have measured the magnetoelectric current of single crystals of CDC for  $H \parallel c$  with the polarization  $P \parallel b$  down to  $^3\text{He}$  temperatures in the 50 T short pulse magnet at NHMFL-LANL. The rapid rise time of this magnet was necessary to increase the signal to noise of the magnetoelectric current in this sample.

### RESULTS AND CONCLUSION

Our magnetoelectric measurements (Figure 2) indicate that ferroelectricity occurs in the same region of  $H$ - $T$  space as the AFM B phase between  $0.35 \text{ T} < H < 4 \text{ T}$  and below  $T = 0.93$  K. Hysteresis is observed in the polarization depending on the direction of the previous two field sweeps. Interestingly, we find the same results with and without electrically poling the sample. The spin polarization calculated from the magnetoelectric current closely tracks the magnetic order parameter. While the magnetically-induced ferroelectricity in CDC is far from practical temperatures and fields, it nevertheless demonstrates that this phenomenon can occur in a whole new class of compounds.

### ACKNOWLEDGEMENTS

This work was supported by the NSF, the DOE, and the state of Florida through the NHMFL and through V.S.Z.'s IHRP grant. Work at JHU was supported by the NSF through DMR-0086210 and DMR-9704257.

### REFERENCES

- [1] R. D. Willett *et al*, *Inorg. Chim. Acta* **4**, 447 (1970); C. P. Landee *et al*, *Phys. Rev. B* **35**, 228 (1987).  
 [2] M. Kenzelmann *et al*, *Phys. Rev. Lett.* **93**, 017204 (2004); Y. Chen *et al*, unpublished (2007).

The experiment is of the fundamental interest: The fully polarized  $^3\text{He}$  has been discussed since the very old days, but the  $^3\text{He}$  Bohr magneton smallness would demand huge magnetic fields for the complete polarization. In Rep 109 the solution of  $^3\text{He}$  in  $^4\text{He}$  formed the degenerate "Fermi gas" at very low temperatures; for a dilute gas the s-wave scattering is the prevailing interaction between  $^3\text{He}$ - $^3\text{He}$  atoms. Once a strong enough magnetic field orients all spins in one direction, the s-wave scattering is excluded due to the Pauli principle. This is the "trick" the authors use for the detection of the fully polarized state in the solution--the mean free path increases and this is seen as the drastic increase in the viscosity.

Fully polarized state dubbed as "the half-metallic" phase is assumed as the ferromagnetic phase of the cubic manganites and some other materials. In that case the proof of the 100% -polarization is far from being so straightforward and so elegant.

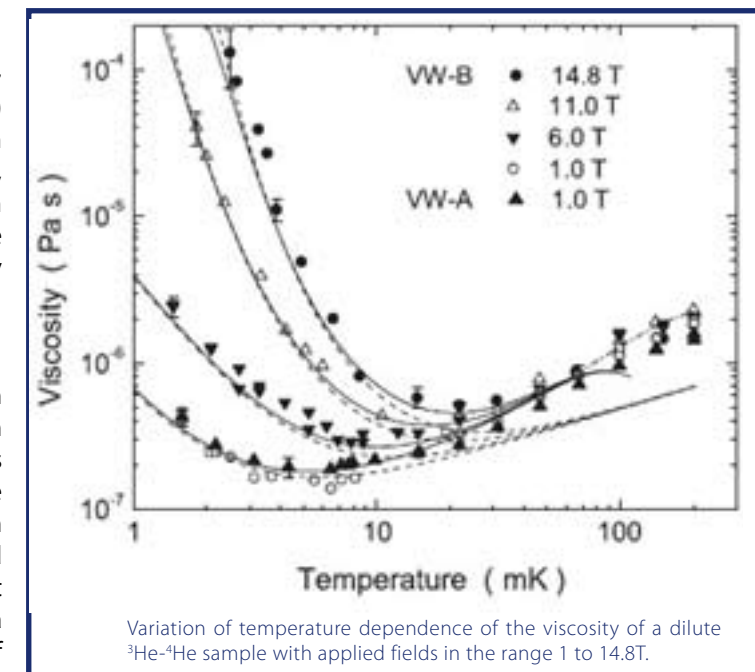
• This work was published in *Physical Review Letters* (2007) and supported by the Magnet Lab's User Collaboration Grants Program.

## GIANT VISCOSITY ENHANCEMENT IN A SPIN-POLARIZED FERMI LIQUID

H. Akimoto (RIKEN, Japan), J. S. Xia (UF-Physics), D. Candela (University of Massachusetts, Physics), W. B. Mullin (University of Massachusetts, Physics), E.D. Adams (UF-Physics), N. S. Sullivan (UF-Physics)

### INTRODUCTION

At extremely high magnetic fields ( $B \sim 14$  T) and low temperatures ( $T \sim 2$  mK) the separation of the spin levels can become greater than the Fermi energy, and the nuclear spin polarization tends to unity. As a consequence the s-wave scattering is strongly suppressed because only antiparallel pairs can scatter in s-wave orbital states and the number of antiparallel pairs drops with increasing spin polarization. The viscosity along with other transport properties depends on the quasiparticle-quasiparticle scattering and its measurement can provide a sensitive test of the predicted suppression of s-wave scattering at very low temperatures. One expects a strong enhancement of the viscosity of Fermi systems for conditions of high  $B/T$ . Dilute  $^3\text{He}$  in liquid  $^4\text{He}$  is an almost ideal sample to test this prediction for experimentally accessible magnetic fields and temperatures.



Variation of temperature dependence of the viscosity of a dilute  $^3\text{He}$ - $^4\text{He}$  sample with applied fields in the range 1 to 14.8 T.

### EXPERIMENTAL

In a previous study<sup>1</sup> at the NHMFL High B/T facility, pulsed NMR was used to demonstrate the existence of a novel damping of spin currents in  $^3\text{He}$ - $^4\text{He}$  mixtures. In this new study<sup>2</sup> a special composite vibrating-wire was used to measure the momentum transport (viscosity) in  $^3\text{He}$ - $^4\text{He}$  mixtures under similar high B/T conditions. Here we summarize the reports of results for measurements of the viscosity using a vibrating wire at very low temperatures ( $2 < T < 100$  mK)<sup>2</sup>. The required experimental conditions were met using the nuclear demagnetization refrigerators of the NHMFL High B/T facility.



Samples were prepared from gaseous mixtures to have 200ppm  $^3\text{He}$  concentrations. Careful NMR calibration measurements at low temperatures established that the condensed samples in the low temperature cells contained 150 ppm  $^3\text{He}$ , the difference with the gas concentration being attributed to surface absorption during the condensation process.

### RESULTS AND DISCUSSION

The results of the viscosity measurements are shown in Figure 1. The data shows the exponential increase of the viscosity for high spin polarizations; i.e. for  $T < 10$  mK and  $B > 11$  T. The results can be used to test theories of transport in degenerate, highly polarized Fermi liquids, and in particular test the current models for quasiparticle interactions in  $^3\text{He}$ - $^4\text{He}$  mixtures which are mediated by phonon exchange.

### CONCLUSIONS

The giant enhancement of the viscosity of a prototype dilute Fermi system has been demonstrated experimentally for 150 ppm  $^3\text{He}$  in liquid  $^4\text{He}$ . The quantitative dependence is in good agreement with the expected dependence on polarization estimated from current models of quasiparticle-quasiparticle scattering at low temperatures.

### REFERENCES

- [1] Akimoto H., *et al.*, *Phys. Rev. Lett.* **90**, 105301 (2003).  
 [2] Akimoto H., *et al.*, *Phys. Rev. Lett.* **99**, 095301 (2007).

In samples of Ge implanted with Mn (concentrations of 3% and 6%) the authors have found huge magnetoresistance at temperatures around  $\sim 30$ K. The effect is so large that, according to the report, it can be described as a transition from a "metallic" state (below 10T) to an insulator-like state at higher fields in this temperature range. Interesting results were also found for the Hall effect. As it is known, the latter in a magnetic substance has two components: the normal Hall coefficient stands in front of the linear dependence on the applied magnetic field; the second component called as the Extraordinary Hall Effect (EHE) is proportional to the magnetization. Measurements in the broad enough range of magnetic field have revealed that the large magnetic field suppresses EHE. Therefore the Hall resistivity discloses the pronounced non-monotonous dependence on the field. The mechanisms responsible for this unique feature remain unknown.

• This work was supported by the Magnet Lab's Visiting Scientist Program.

## HIGH FIELD MAGNETOTRANSPORT IN Mn IMPLANTED Ge

A. Gerber, O. Riss (School of Physics, Tel Aviv University, Israel), and A. Suslov (NHMFL)

The giant and colossal magnetoresistivity (GMR/CMR) remains one of the hot topics in the condensed matter physics during the last two decades because of the great variety of potential and already realized applications (magnetic recording, magnetic field sensors, etc.) and due to many fundamental problems which arise in the course of the study of various aspects of this multifaceted phenomenon. There are three main classes of systems, in which the electrical resistivity changes by the order of magnitude or even more in an external magnetic field: (i) multilayered systems containing ferromagnetic layers separated by non-magnetic metallic layers (ii) granular nanocomposites containing magnetic granules; (iii) transition metal and rare-earth oxides, in which the electron transport is sensible to external magnetic field in the vicinity of structural, metal-insulator and magnetic field induced transitions as well as charge and orbital ordering phenomena. The mechanisms of the field enhancement or suppression of the magnetic scattering in these three systems are different, and one may anticipate that other mechanisms of (GMR/CMR) may act in other types of materials with nanoscale inhomogeneity.

This work is devoted to magnetotransport in germanium heavily doped by Mn. Magnetoresistance and Hall effect were measured in two samples with Mn concentration of 3% and 6% in fields up to 33 T and temperatures down to 4.2 K at the National High Magnetic Field Laboratory. Selection of magnetoresistance and Hall resistance at several temperatures is presented in Figures 1a and b.

Magnetoresistance depends strongly on temperature. It is relatively small at 4.2 K, but grows to thousands of percents around 30 K with the further reduction at higher temperatures. Magnetic field driven metal-insulator transition takes place at fields of about 10 T with metallic state at lower fields and insulator-like state at high fields. Magnetoresistance rise is very sharp below 20 K where the zero field metal-insulator transition takes place as a function of temperature.

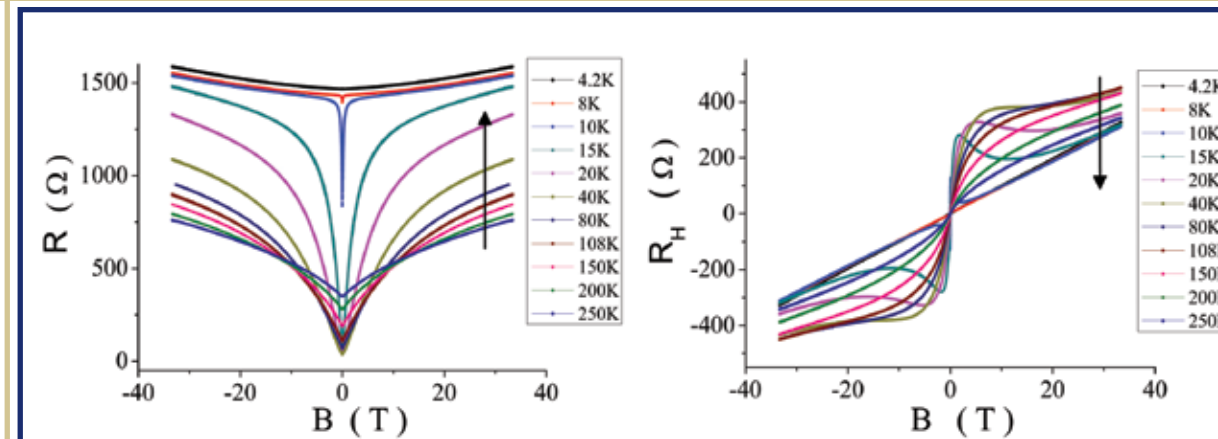


Figure 1.

Magnetoresistance (a) and Hall effect (b) of MnGe sample with 3% Mn at different temperatures. Arrows indicate the reduction of temperature.

Hall effect data is not less puzzling. Both the ordinary and the Extraordinary Hall effects (EHE) contribute to the shape and magnitude of the Hall resistance. The EHE component is usually generated by spin orbit scattering by magnetic impurities and ferromagnetic clusters embedded in a conducting matrix. The remarkable feature shown in the figure is suppression of the EHE by magnetic field, resulting in a non-monotonous field dependence. To the best of our knowledge this is the first observation of such phenomenon.

### ACKNOWLEDGEMENTS

Experiments at NHMFL were supported in part by NHMFL Visiting Scientist Program.

The manipulation and extended study of the properties of one of nature's most interesting structures, the carbon nanotube, is rapidly becoming important to many areas of technology, not the least of which is energy. With many important energy related applications of carbon nanotubes requiring controlled, scalable production of large quantities, this Highlight provides a new tool for control of some properties of large quantities of carbon nanotubes based on NHMFL-level magnetic fields.

## ELECTRICAL AND MECHANICAL PROPERTIES OF MAGNETIC-FIELD ALIGNED SINGLE-WALLED CARBON NANOTUBE BUCKYPAPERS

J.G. Park, X. Fan, S. Li, R. Liang, C. Zhang, B. Wang (FSU, HPMI); J.S. Brooks (FSU, Physics)

### INTRODUCTION

Carbon nanotube (CNT) is fascinating lightweight material recognized for its low dimensionality with high electrical and thermal conductivity and excellent mechanical properties. Sheets of nanotubes or nanofibers, known as buckypaper (BP), provide a promising medium to control the properties of CNT. Several methods, such as alignment under magnetic<sup>1</sup> or electric fields, e-beam or ion beam irradiation<sup>2</sup>, are under investigation to improve the electrical and mechanical properties of BP to produce high-performance nanocomposites. In this research, magnetically aligned BPs up to  $10'' \times 10''$  were produced and tested to determine their electrical and mechanical properties as a function of magnetic field.

### EXPERIMENTAL

Purified Hipco SWCNT (Carbon Nanotechnologies Inc., TX) was dispersed in an aqueous solution. To align the CNTs, BPs were produced under different magnetic fields up to 17.3 T. The aligned BP samples were cut in rectangular shapes for electrical and tensile tests. Polarized Raman with 785 nm excitation (0.5 mW) was used to check alignment. Electrical conductivity was measured using a conventional four-probe method. Tensile strength and modulus were measured in a dynamic mechanical analyzer (DMA 2980, TA instruments).

### RESULTS AND DISCUSSION

Figure 1 shows normalized G band intensities of aligned BPs from polarized Raman indicating alignment increased as the magnetic field increased. As shown in Figure 2, electrical conductivity was enhanced by more than four times for BP produced in higher magnetic fields. Conductivity anisotropy,  $\sigma_{\parallel} / \sigma_{\perp}$ , also increased

along with magnetic field strength. Mechanical properties improved as a result of magnetic alignment. Figure 3 shows tensile modulus and strength of aligned BPs increased by more than factor of two.

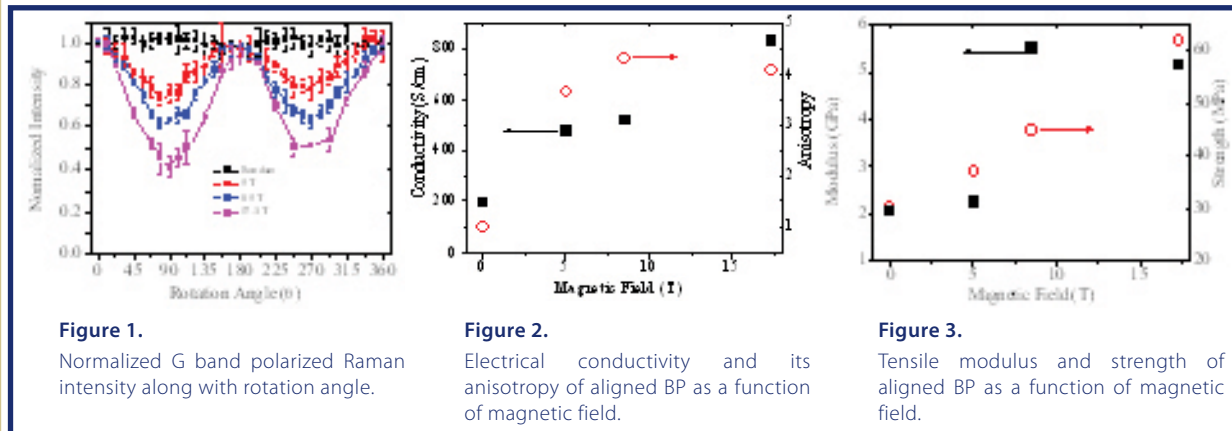


Figure 1.

Normalized G band polarized Raman intensity along with rotation angle.

Figure 2.

Electrical conductivity and its anisotropy of aligned BP as a function of magnetic field.

Figure 3.

Tensile modulus and strength of aligned BP as a function of magnetic field.

## CONCLUSIONS

BP production under magnetic fields enhances the CNT alignment, which improves the electrical and mechanical properties. CNT alignment improves as a function of the magnetic field strength, enhancing electrical and mechanical properties of BP by more than factor of two-four. These improvements should facilitate producing high performance composites.

## REFERENCES

- [1] Fischer, J. E., *et al.*, *J. Appl. Phys.* **93**, 2157 (2003).
- [2] Krasheninnikov, A. V., *et al.*, *Nature Mat.*, **6**, 723 (2007).

Three-terminal devices with conduction channels formed by quasi-metallic carbon nanotubes (CNTs) are shown to operate as nanotube-based field-effect transistors under strong B (up to 30 T). An exponential decrease of the device off-state conductance is observed under high axial B up to room temperature, and it is attributed to the opening of an energy gap in the CNT electronic spectrum. Remarkably, under high axial B the devices operate as CNT FETs with the on/off conductance ratio exceeding  $10^4$ .

The temperature dependent magnetotransport is also shown to be a new tool to determine the quasi-metallic nanotube chirality.

• This work was published in *Nano Letters* (2007) and was supported by the Magnet Lab's User Collaboration Grants Program.

## EXPLORING THE MAGNETICALLY INDUCED FIELD EFFECT IN CARBON NANOTUBE BASED DEVICES

G. Fedorov (NHMFL), A. Tselev (Georgetown University), D. Jimenez (University of Barcelona, Spain), S. Latil (University of Namur, Belgium), N. Kalugin (New Mexico Tech), P. Barbara (Georgetown University), D. Smirnov (NHMFL) and S. Roche (CEA, France)

The exceptional low-dimensionality and symmetry of carbon nanotubes (CNT) are at the origin of their spectacular physical properties governed by quantum effects. Ajiki and Ando<sup>1</sup> predicted that an axial magnetic field would tune the band structure of a CNT between a metal and a semiconductor, owing to the modulation of the Aharonov-Bohm (AB) phase of the electronic wave functions. Here we report on a high magnetic field study of the AB-effect on transport properties of gated (quasi)-metallic single wall carbon nanotubes (SWCNTs)<sup>2</sup>.

The magnetotransport measurements were conducted using devices made in the configuration of a standard CNT field-effect transistor (CNFET), as shown in Figure 1. The conductance characteristics  $G(V_g)$  were recorded at temperatures from 1.5 K to 290 K and in magnetic fields up to 30 T.

Figure 2 shows the conductance of a CNFET device 1 made with a quasi-metallic CNT, measured at the coaxial magnetic field. Perpendicular magnetic fields do not significantly change the conductance. Suppression of the conductance around  $V_g^*$  indicates the presence of the narrow gap in a quasi-metallic CNT at  $B=0$ . As the axial magnetic field increases, the gap decreases to reach a minimum value at  $B_0 \sim 6$  T. Device 2 behaves as

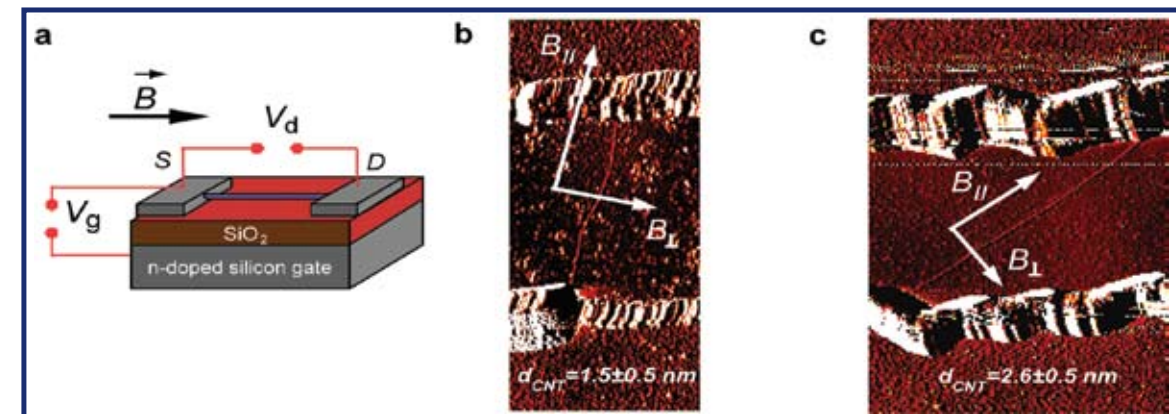


Figure 1.

(a) Schematic of a CNFET type device. (b), (c) AFM images of two studied CNFET devices. White arrows indicate direction of the magnetic field.

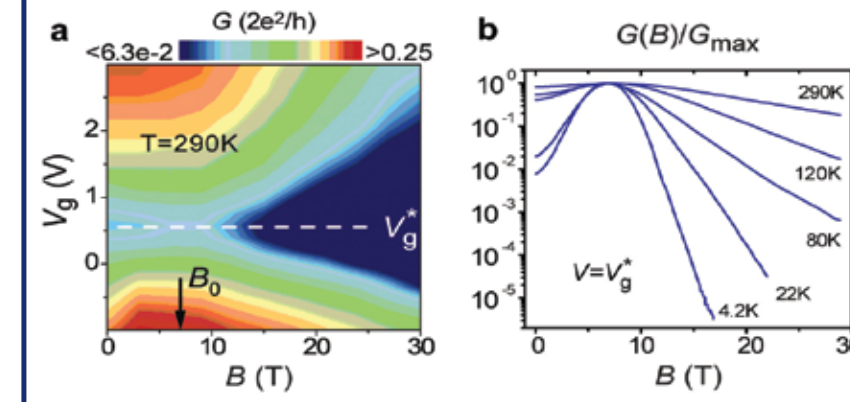


Figure 2.

(a) Plot of the sample 1 conductance versus the gate voltage and the axial magnetic field. A dark arrow indicates the value of  $B_0$ , where  $\epsilon_g(B)$  has a minimum. (b) Off-state magnetoconductance of sample 1.

a truly metallic nanotube with  $B_0 \sim 0$  T. Above  $B_0$ , a region of suppressed conductance develops, indicating a monotonous increase of a band gap in both samples. Remarkably, under high axial magnetic fields the devices operate as CNFETs with the on/off conductance ratio exceeding  $10^4$ .

Qualitatively, the experimental observations agree with the predicted  $\epsilon_g(B)$  dependence, and therefore strongly favor the interpretation of our data in terms of the AB effect. A quantitative picture of CNFET magnetoconductance is achieved in the frames of a model incorporating both the AB effect on the bandstructure of the nanotubes and the AB effect on the barriers formed at the nanotube/contact interface

To summarize, we report on observation of a magnetic field induced conversion of initially metallic carbon nanotube devices into carbon nanotube field effect transistors. Strong exponential magnetoresistance observed up to room temperature is the ultimate consequence of the linear increase of the band gap with a magnetic field. The magnetic field controlled Schottky barriers significantly contribute to the CNT magnetoconductance, which may suggest new routes to engineer CNT-based devices characteristics. Moreover, this study reveals the temperature-dependent CNT magnetotransport as a new tool to explore the symmetries of carbon nanotubes.

## ACKNOWLEDGMENTS

Financial support of this work was provided by NHMFL In House Research Program, Ministerio de Educacion y Ciencia under project TEC2006-13731-C02-01/MIC and NSF (DMR 0239721).

## REFERENCES

- [1] H. Ajiki and T. Ando, *J. Phys. Soc. Jpn.* **62**, 1255 (1993)
- [2] G. Fedorov, *et al.*, *Nano Letters*, **7**, 960 (2007).



Angular dependent resistivity measurements of optimally doped YBCO films in B pulsed up to 50 T provide the first evidence for the presence of the liquid-crystalline smectic phase predicted for layered superconductors. In particular, when B is aligned with the layers, the rapid increase of the vortex melting field at low temperatures and the critical exponent analysis confirm the presence of the smectic. They also observe that, up to the highest B applied (50 T), correlated defects arrest the motion of vortices well into the liquid phase.

• This work was published in *Physical Review Letters* (2007) and was supported by the Magnet Lab's User Collaboration Grants Program.

## SMECTIC VORTEX PHASE AT HIGH FIELDS IN OPTIMALLY DOPED HIGH-TEMPERATURE SUPERCONDUCTOR

S. A. Baily, B. Maiorov (NHMFL/STC, LANL); F. F. Balakirev, M. Jaime (NHMFL, LANL); H. Zhou, S. R. Foltyn, L. Civale (STC, LANL)

### INTRODUCTION

Deep into the superconducting state when a magnetic field is applied it penetrates creating vortices, that can exist in solid, liquid, phases. The nature of these phases is given by the nature of pinning center present.<sup>1</sup> Also, pinning centers enable films to carry more current is an extremely important for applications of superconductivity. The most interesting case occurs along the copper oxide planes of HTS where all kinds of pinning centers are present.<sup>2</sup> When the magnetic field, or temperature increases the vortex lattice crosses the melting line and becomes a liquid with the concomitant increase of the electrical resistance.

### EXPERIMENTAL

Electrical ac-transport was used to measure the vortex dissipation in the liquid phase as well as to determine the melting line (where dissipation goes to zero), as a function of angle for  $\text{YBa}_2\text{Cu}_3\text{O}_7$  (YBCO) films in the 50 T short-pulse magnet using the newly rebuilt rotator probe. The effect of naturally grown defects on the melting line was studied, in particular for the defects along the ab-planes.

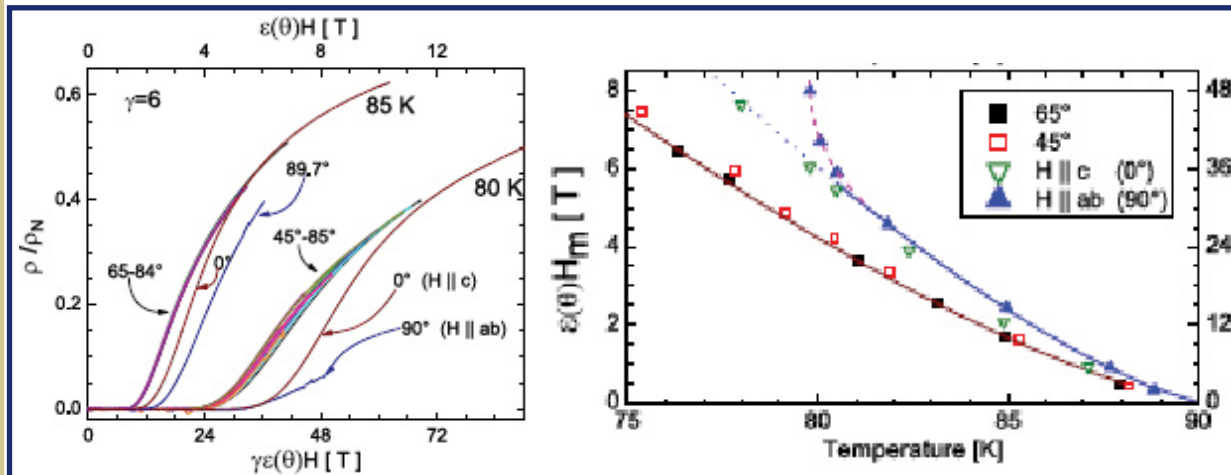


Figure 1.

Left: Normalized resistance vs. scaled field at two temperatures. Right:  $\epsilon(\theta)H$  vs. Temperature with the magnetic field applied at different orientations.

### RESULTS AND DISCUSSION

We find that near 80 K ( $H > 40$ T), when the magnetic field is aligned with the layers, the melting line has an upward turn and the critical exponent that describes the rise in resistivity upon entering the liquid state becomes similar to that of the liquid crystal transition predicted for layered superconductors. Also we observe that up to the highest field measured (50 T) correlated defects arrest the motion of vortices well into the liquid phase.

### CONCLUSION

A long-standing debate about the existence of a smectic vortex phase in "low anisotropy" high-temperature

superconductor been settled, with the evidence for smectic vortex phase in optimally doped YBCO at fields higher than 40 T, available with pulsed field.<sup>3</sup>

### ACKNOWLEDGEMENTS

This work was supported by the NSF through the NHMFL and NHMFL IHRP, the State of Florida and the DOE.

### REFERENCES

- [1] G. Blatter, *et al.*, *Rev. Mod. Phys.* **66**, 1125 (1994).
- [2] L. Balents and D. R. Nelson, *Phys. Rev. Lett.* **73**, 2618 (1994).
- [3] S.A. Baily *et al.*, *Physical Review Letters* (Accepted for publication).

$\text{CeIn}_3$  has the cubic structure. It is the f-electron antiferromagnet with a considerable hybridization. Changes in the Fermi surfaces' sizes under applied pressure or in high magnetic field seen by means of the dHvA experiment provide information about competition between itinerancy and the degree of localization of the Ce f-electrons. The electronic properties of  $\text{CeIn}_3$  for the polarized phase that sets in at strong magnetic fields and the paramagnetic phase at the pressure above the critical pressure  $\sim 25$  kbar are different. In the magnetic fields above  $\sim 60$  T the f-electrons do not contribute to the Fermi surfaces' volume. The effective masses get reduced to the values of few free electron masses and do not vary with the field increase. This research is the significant technical breakthrough in the use of the pulsed magnetic fields for the scientific experiments and contains interesting new results concerning  $\text{CeIn}_3$ .

• This work was published in *Physical Review Letters* (2007).

## MEASUREMENTS ON $\text{CeIn}_3$ IN NON-DESTRUCTIVE 100 TESLA MAGNET FIELDS

N. Harrison (NHMFL, LANL), C. H. Mielke (NHMFL, LANL), S. E. Sebastian (Cambridge U., Physics), T. Ebihara (Shizuoka Univ., Physics)

Scientists have long since been able to subject materials to the extremes of magnetic field beyond 100 tesla, utilizing explosive flux compression or singleturn coil techniques. The destruction of the sample by the explosively driven systems is not an option for many "one-of-a-kind" or otherwise "valuable" samples. For conductors, however, the rapid rates of change of magnetic flux brought on by their microsecond duration proves to be an additional experimental hurdle to conquer. If not addressed the Joule heating caused by the induced eddy currents will raise the temperature of the sample significantly.

To counteract these problems, high magnetic field scientists around the world have for the past two decades been attempting to generate magnetic fields approaching 100 tesla in a controlled fashion, non-destructively, with millisecond duration. The demands on material strength and electrical energy have proven to be much more of a challenge than previously

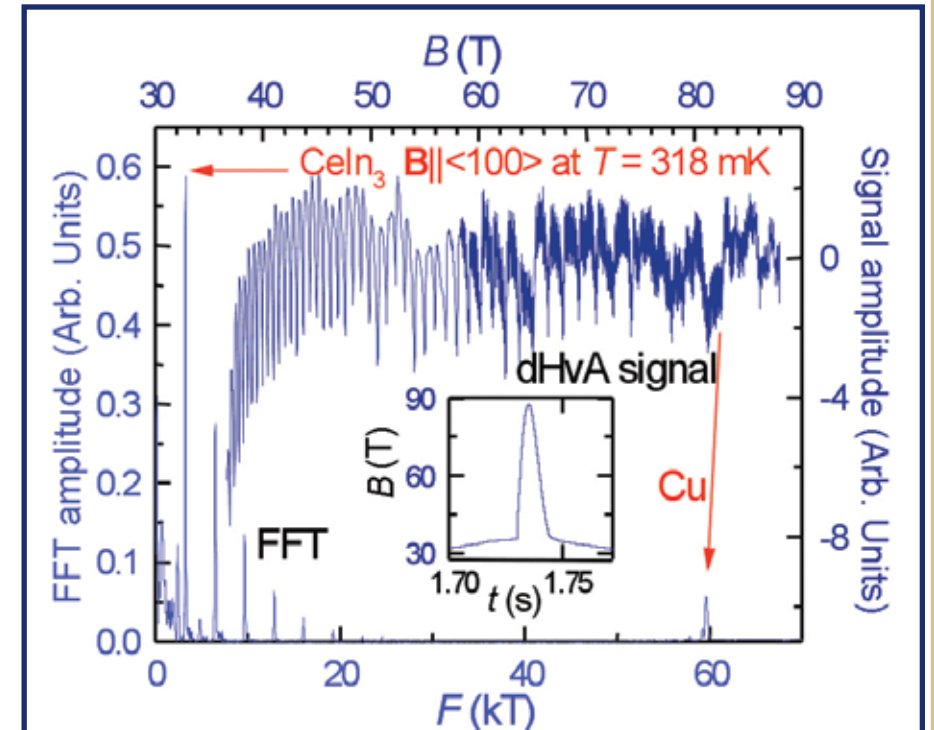


Figure 1

The raw dHvA signal in  $\text{CeIn}_3$  and the spectral analysis. (Inset) The Magnetic Field pulse near peak field showing the  $\sim 35$  tesla platform field.

anticipated. Only recently have controlled magnetic fields anywhere near 100 tesla become close to being realized. A team of scientists and engineers at the Los Alamos branch of the NHMFL have commissioned a 100 tesla multishot magnet with the intention of providing slightly reduced magnetic fields of  $\sim 90$  T for experimental use in an interim period before the frontiers are finally pushed back to their ultimate goal. These World Record millisecond pulsed fields reach approximately 30 tesla beyond what was previously available for experiments in pulsed magnetic field laboratories— opening the door for countless new opportunities.

$\text{CeIn}_3$  provides the first example of a system, in which temperatures of  $\sim 318$  mK (3/10 of a degree above absolute zero) enable observation of the quantum oscillations in the magnetization, better known as the de Haas van Alphen (dHvA) effect. Figure 1 shows an example of raw data of such oscillations measured in a pulse extending to 88 tesla. The Fourier transform of the oscillations in Figure 2 (done in reciprocal magnetic field) provides a reliable in-situ calibration of the magnetic field; the fundamental dHvA frequency  $F \sim 59.5$  kT of Cu originates from the windings of the detection coil while that of  $F \sim 3.22$  kT corresponds to a sample of  $\text{CeIn}_3$  aligned with the field is parallel to its  $\langle 100 \rangle$  axis.

$\text{CeIn}_3$  is of interest because it belongs to a small family of Ce-based antiferromagnets that become superconducting under the application of hydrostatic pressure, just at the point where antiferromagnetic order is suppressed<sup>1</sup>. Knowledge on the degree to which the f-electrons contribute to the electrical properties throughout is an essential prerequisite for understanding the origin of unconventional superconductivity. Strong magnetic fields assist in our pursuit of this understanding by changing the extent to which the f-electrons contribute to electrical conduction by polarizing their spin degrees of freedom. This polarization depletes the system of available spin degrees of freedom for ordering, causing the antiferromagnetic order to be suppressed (as under pressure). This then manifests itself by way of subtle changes in the electronic structure that can be observed as field-induced changes in the dHvA Fourier spectrum. This work was jointly supported by the NSF, DOE, and Florida State.

#### REFERENCES

[1] Harrison, N., *et al.*, Physical Review Letters 99, 056401 (2007).



# NATIONAL HIGH MAGNETIC FIELD LABORATORY

Supported by:

THE NATIONAL SCIENCE FOUNDATION  
and the  
STATE OF FLORIDA

1800 EAST PAUL DIRAC DR.  
TALLAHASSEE, FL 32310-3706  
850.644.0311  
[www.magnet.fsu.edu](http://www.magnet.fsu.edu)

Operated by:

FLORIDA STATE UNIVERSITY  
UNIVERSITY OF FLORIDA  
LOS ALAMOS NATIONAL LABORATORY

